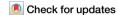


https://doi.org/10.1038/s40494-025-01861-1

# Early degradation mechanisms at the interface between acrylic grounds and oil paint films



Margherita Gnemmi<sup>1,2</sup>, Laura Fuster-L-ópez³⊠, Miguel Ángel Herrero-Cortell³, Angel Vicente-Escuder⁴ & Francesca Caterina Izzo¹⊠

This research was aimed to identify, localize and characterize degradation phenomena such as wrinkles, protrusions and cracks at their earliest stages of formation in contemporary oil paintings, even before they become visible to the naked eye, and with a special focus on the failure mechanisms taking place at the interface between oil paint films and acrylic-based grounds. Multiband imaging provided detailed information on the nature and distribution of degradation phenomena across the entire stratigraphy. These findings were then compared and validated at the morphological and elemental level by HR-FESEM-EDX. ATR-FTIR spectroscopy provided further insight into the organic components and potential degradation products on the surface, while GC-MS identified and quantified organic compounds, providing evidence of oxidation and hydrolysis reactions occurring in the bulk. This approach evidences how informative multiband imaging can be in providing valuable insights into degradation phenomena and in assisting in the design of the experimental strategy.

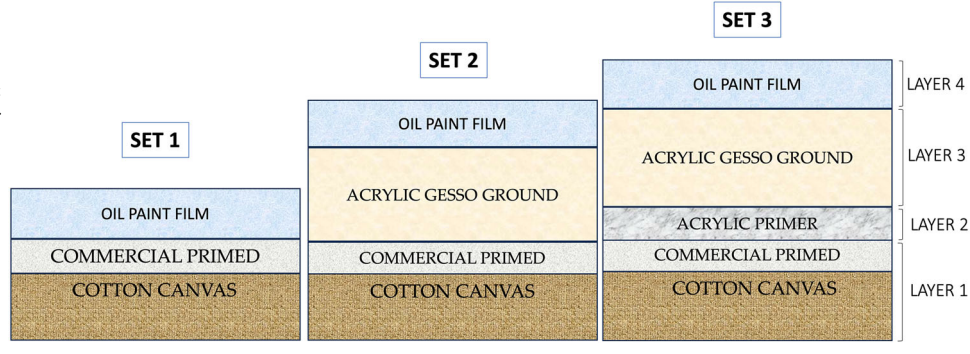
In the 1950s, the advent of acrylic dispersion paints transformed the production of grounds<sup>1-3</sup>. The first acrylic-based paints were introduced by Liquitex in 1955. The term "gesso" was adopted by early manufacturers, such as Bocour, Bourgeois Lefranc and Liquitex, among others, to describe acrylic grounds<sup>4,5</sup>. During the 1970s and 1980s, oil-primed canvases gradually gave way to acrylic-primed ones, and in 1975-76, Winsor & Newton introduced acrylic grounds on cotton canvases, which are still the most widely used ones by artists today<sup>6,7</sup>. Many manufacturers now favor acrylic grounds due to their versatility, cost-effectiveness, and fast-drying properties, making them more efficient to produce. There are two main types of acrylic grounds available nowadays in the market: "acrylic primers" and "acrylic gesso grounds". Both are used indistinctly in preparatory layers. However, previous research showed that acrylic primers contain a lower concentration of extenders than acrylic gesso grounds<sup>8-10</sup>. Acrylic gesso grounds typically contain a water-based acrylic emulsion. This is usually a copolymer resin of ethyl acrylate/methyl methacrylate (EA/ MMA) or butyl acrylate/methyl methacrylate (BA/MMA), although other monomers such as styrene may also be present<sup>11</sup>. Polymer droplets are dispersed in water in an "emulsion base" (or "base dispersion"), which is unpigmented and stabilized with surfactants, antifoams, etc. Various additives such as thickeners, dispersing agents, freezing agents, and coalescing solvents are added during production. Titanium white  $(TiO_2)$  is typically used as the pigment in acrylic grounds, while gypsum, barium sulphate, calcium carbonate, kaolin, talc, and silica can be added as extenders to achieve the desired pigment volume, surface roughness, and porosity/absorbency of the film $^{12-14}$ .

Paintings made in the 20th and 21st centuries are complex systems where organic and inorganic materials coexist as a function of artists' choices and preferences<sup>15–19</sup>. The use of oil paint on ready-to-use acrylic preprimed commercial canvases has been a common practice, offering versatility and fast-drying times. However, the interaction between these two layers remains insufficiently understood, particularly at their interface. While acrylic grounds are appreciated for their rapid drying and flexible nature, they have been reported to cause delamination and degradation in some instances, raising concerns about their long-term stability when combined with oil-based paints<sup>7,12,17,20</sup>.

The existing literature on delamination issues at the interface between synthetic grounds and oil paint films remains scarce. A study on selected O'Keeffe's paintings explored the hypothesis that the formation of protrusions on the surface of her paintings was linked to changes in her painting technique<sup>21,22</sup>. In a specific period of her career, O'Keeffe used pre-primed commercial canvases that contained white pigments and fillers such as lead white, barium white, zinc white

<sup>1</sup>Ca' Foscari University of Venice, Department of Environmental Sciences, Informatics and Statistics, Venice, Italy. <sup>2</sup>Sapienza University of Rome, National PhD in Heritage Science, Rome, Italy. <sup>3</sup>Universitat Politècnica de València, Instituto Universitario de Restauración del Patrimonio, Valencia, Spain. ⁴Universitat Politècnica de València, Instituto de Tecnología de los Materiales, Valencia, Spain. ⊠e-mail: laufuslo@crbc.upv.es; fra.izzo@unive.it

Fig. 1 | Stratigraphy of the sets of mock-ups prepared. SET1: commercial primed cotton canvas + oil paint film; SET2: commercial primed cotton canvas + acrylic gesso ground + oil paint film; SET3: commercial primed cotton canvas + acrylic primer + acrylic gesso ground + oil paint film.



and calcium carbonate, often modified with plasticizers and other additives<sup>23–27</sup>. A possible interaction between the acrylic ground and the oil paint layers was investigated, but the main cause of the protrusion formation was attributed to the presence of lead white<sup>28–31</sup>.

Recently, the formation of cracks on canvases featuring acrylic gesso grounds and oil paint layers, particularly those containing titanium dioxide ( $\text{TiO}_2$ ) or zinc oxide (ZnO) with lipid-based binders, has been reported<sup>4,11,14,20,32</sup>.

Specific literature reports that paint layers composed primarily of zinc oxide become increasingly stiff and brittle within a few years after application  $^{33-38}$ 

Furthermore, it has been observed that internal fractures and cracks developed already during the early stages of drying in oil paintings on acrylic grounds  $^{33-37}$ .

Conversely, while previous studies have linked this degradation to factors such as film thickness, fluctuations in relative humidity and temperature, and physical impacts<sup>12–14,39</sup>, the specific degradation mechanisms resulting from the interaction between an oil paint film and an acrylic gesso ground have not been thoroughly investigated.

The present study focuses on the interaction between ground and paint layers, analyzing the dynamic and evolving nature of painting materials, considered as systems in constant change. The research builds up on a recent study focused on the migration of metal ions and the degradation mechanisms observed in oil paint films, examining the early stages of drying and long-term stability<sup>40,41</sup>. Through a hybrid experimental approach, both vertical and transverse ion migration were investigated in adjacent oil paint films containing different sources of metal ions (e.g., pigments). Key findings highlighted the role of metal ions in influencing drying rates, reactivity, and structural changes in oil paint films, such as cracking, delamination, and protrusions, often linked to the chemical and physical properties of specific pigments. A deeper understanding of the interaction between the pictorial layers was provided. This led to a shift in focus from the adjacent to the overlapping pictorial layers, allowing the interactions between all structural levels to be examined rather than limiting the analysis to the pictorial layer alone.

This study is one of the first to illustrate the potential of multiband imaging (MBI) not only for the preliminary identification of pigments in works of art but also capable of detecting and localizing degradation phenomena invisible to the naked eye.

This research provides an analytical protocol that combines a non-invasive, in situ technique such as MBI with advanced morphological and elemental techniques such as FESEM-EDX, ATR-FTIR, and GC-MS to compare, validate and explore organic components and degradation products in both surface and bulk layers. This comprehensive protocol will firstly provide artists with informed guidance on the appropriate selection and combination of materials and secondly, a non-invasive methodology for implementing preventive conservation strategies for contemporary paintings.

# **Methods**

#### Sample preparation

In order to gain a deeper insight into the materials most used by artists today, a survey was carried out among 32 Italian artists, both amateurs and professionals. They provided information on:

• Materials:

The most commonly used support was 100% cotton canvas, typically pre-stretched and pre-primed. The technical data sheets for these canvases often specify a ground consisting of highly pigmented titanium dioxide with an acrylic binder.

Artists often add additional acrylic gesso grounds and acrylic primers when using oil-based paint films, being Winsor & Newton (W&N) and Golden Artist Color Inc. the most commonly used brands, respectively. Maimeri and W&N oil paints were the most used.

 Degradation issues: several artists reported issues such as cracking, wrinkling and delamination, particularly in white paint areas or colors mixed with zinc and titanium whites, even after the first few days in some cases.

The preparation of the representative mock-ups was informed by the survey and reflects the typical layered structure found in Italian contemporary paintings. Figure 1 illustrates the stratigraphy of the different sets of mock-ups prepared.

Three sets of mock-ups were cast.

- SET1 consisted of two layers: commercial primed cotton canvas + oil paint film.
- SET2 consisted of three layers: commercial primed cotton canvas + acrylic gesso ground + oil paint film.
- SET3 consisted of four layers: commercial primed cotton canvas + acrylic primer + acrylic gesso ground + oil paint film.

The samples were prepared according to different combinations with the following materials:

- A commercial primed medium weave 100% cotton canvas (300 g/m²) produced by Canvaslot. The technical data sheets specify that the canvas was stretched and secured with lateral staples on a  $17 \times 38$  mm stretcher made of spruce bars.
- An acrylic gesso ground: Winsor & Newton acrylic gesso ground
- An acrylic primer Golden acrylic primer
- An oil paint film: two different oil paint films were selected (zinc white and titanium white) produced by three different brands (Maimeri, Williamsburg for Golden Artist Color Inc., Winsor & Newton)

(Table 1).

The preparatory and paint layers were applied using a spatula by the same operator, who maintained constant pressure to ensure uniform thickness across all samples.

The thicknesses of each layer, measured by the HR-FESEM-EDX instrument, are shown below through an average of 20 cross-sectional

Table 1 | Summary of the sets of mock-ups prepared.

SUPPORT	PREPARATORY LAYERS(S)		OII PAINT FILM			AGING
	Level 1	Level 2				
SET1						
Commercial primed cotton canvas			Titanium white	Maimeri	SET1-TiMM	SET1-TIMM-NAT
						SET1-TiMM-RH%
						SET1-TiMM-T
				Golden	SET1- TiGD	SET1- TiGD-NAT
						SET1- TiGD-RH%
						SET1- TiGD
				W&N	SET1-TiW&N	SET1-TiW&N-NAT
						SET1-TiW&N-RH%
						SET1-TiW&N-T
			ZINC WHITE	Maimeri	SET1- ZnMM	SET1- ZnMM-NAT
						SET1- ZnMM-RH%
						SET1- ZnMM-T
				Golden	SET1-ZnGD	SET1-ZnGD-NAT
						SET1-ZnGD-RH%
						SET1-ZnGD-T
				W&N	SET1- ZnW&N	SET1- ZnW&N-NAT
						SET1- ZnW&N-RH%
						SET1- ZnW&N-T
SET2						
Commercial primed cotton	Golden acrylic primer		Titanium white	Maimeri	SET2-TiMM	SET2-TiMM-NAT
canvas						SET2-TiMM-RH%
						SET2-TiMM-T
				Golden	SET2- TiGD	SET2- TiGD-NAT
						SET2- TiGD-RH%
						SET2- TiGD-T
				W&N	SET2- TiW&N	SET2- TiW&N-NAT
						SET2- TiW&N-RH%
						SET2- TiW&N-T
			ZINC WHITE	Maimeri	SET2- ZnMM	SET2- ZnMM-NAT
						SET2- ZnMM-RH%
						SET2- ZnMM-T
				Golden	SET2- ZnGD	SET2- ZnGD-NAT
						SET2- ZnGD-RH%
						SET2- ZnGD-T
				W&N	SET2- ZnW&N	SET2- ZnW&N-NAT
						SET2- ZnW&N-RH%
						SET2- ZnW&N-T
SET3						
Commercial primed cotton canvas	Golden acrylic primer	W&N acrylic gesso ground	Titanium white	Maimeri	SET3-TiMM	SET3-TiMM-NAT
						SET3-TiMM-RH%
						SET3-TiMM-T
				Golden	SET3- TiGD	SET3- TiGD-NAT
						SET3- TiGD-RH%
						SET3- TiGD-T
				W&N	SET3- TiW&N	SET3- TiW&N-NAT
						SET3- TiW&N-RH%
						SET3- TiW&N-T
			Zinc white	Maimeri	SET3- ZnMM	SET3- ZnMM-NAT
						SET3- ZnMM-RH%

Table 1 (continued) | Summary of the sets of mock-ups prepared.

SUPPORT	PREPARATORY LAYERS(S)		OII PAINT FILM			AGING
	Level 1	Level 2				
						SET3- ZnMM-T
				Golden	SET3- ZnGD	SET3- ZnGD-NAT
						SET3- ZnGD-RH%
						SET3- ZnGD-T
				W&N	SET3- ZnW&N	SET3- ZnW&N-NAT
						SET3- ZnW&N-RH%
						SET3- ZnW&N-T

SET1: (commercial primed cotton canvas + oil paint film); SET2: (commercial primed cotton canvas + acrylic gesso ground + oil paint film); SET3: (commercial primed cotton canvas + acrylic gesso ground + oil paint film); Ti: titanium dioxide in rutile; Zn: zinc oxide; GD: brand Golden; MM: brand Maimeri; W&N: brand Winsor & Newton. T: subjected to artificial ageing with temperature variations. NAT: ageing under room temperature conditions; T: artificial ageing with temperature cycles and stable relative humidity parameters; RH%: artificial ageing with relative humidity cycles and stable temperature parameters.

Table 2 | Climatic parameters for natural and artificial ageing in the climate chamber: summary of the relative humidity percentage (RH%) and temperature (T) values used in the climatic chamber during the artificial ageing process.

TYPE OF AGEING	ABBREVIATION	TEMPERATURE PARAMETERS	RELATIVE HUMIDITY PARAMETERS
Natural ageing	NAT	T = 23 °C	RH% = 47%
Artificial ageing-temperature variation only	Т	Cycles T = 50-26 °C	RH% stabile = 55%
Artificial ageing-only moisture fluctuations	RH%	T fixed = 26 °C	Cycles RH% = 90-40%

NAT: ageing under room temperature conditions; T: artificial ageing with temperature cycles and stable relative humidity parameters; RH%: artificial ageing with relative humidity cycles and stable temperature parameters

samples. The value in brackets corresponds to the relative standard deviation:

The reported values using HR-FESEM-EDX.

- commercial primed cotton canvas: 55 μm (±0.3%);
- acrylic gesso ground: 120 μm (±0.2%);
- acrylic primer: 74 μm (±0.4%);
- oil paint film: 330 μm (±0.5%);

The selected acrylic grounds and oil paints were preliminarily characterized, and all the results are reported in the supplementary material (Figs. S1–S22). The main information necessary for a better understanding of the subsequent analysis is given below, and applies to all the selected brands:

- Titanium white (PW4) oil paints are made of very finely ground rutile titanium dioxide TiO<sub>2</sub> mixed with 10% (normalized average in all paint tubes of titanium white) of zinc, identified by XRF analysis shown in supplementary materials (Figs. S12–S14);
- Zinc white (PW6) oil paints are made from finely ground zinc oxide, ZnO;
- The pigment volume concentration (PVC) value of the selected oil paints, determined with the residual mass using thermogravimetric analysis with differential scanning calorimetry (TG-DSC), is 73.84% (±1.166%);
- The type of oil used in the selected paints is alkali-refined linseed oil in the Golden Artist Color Inc. tubes and safflower oil in the Winsor & Newton and Maimeri tubes;
- All the selected grounds consist of acrylic copolymer emulsion (40–60%), titanium dioxide in rutile form (10–20%), inert fillers such as calcite, silica dioxide, kaolin, calcium sulphate bi-hydrate (10–30%), additives such as surfactants, preservatives, etc. (1–5%).

While a series of the three sets were kept in room conditions (indicated by the abbreviation NAT), the rest were subjected to artificial ageing in a climatic chamber, indicated by the abbreviation T (temperature) or RH% (% relative humidity), depending on the type of artificial ageing they underwent. The parameters (Table 2) of the artificial ageing (temperature

variations and fluctuations in relative humidity percentage) were selected to simulate the conditions that the paintings might experience in environments where variations in temperature and humidity fluctuations are difficult to control. This approach aimed to accelerate the ageing process by providing insights into the behavior of materials under high-stress conditions. Specifically, the climatic chamber parameters were selected based on an extreme average of the seasonal maximum and minimum values of relative humidity percentage and temperature that can be found in museum and domestic indoor environments, not necessarily meant to be dedicated to the conservation of paintings. The artificial ageing protocol was set up to provide a cyclic variation of the selected parameters. The climatic chamber required 20 min to transition from the minimum to the maximum selected temperature or relative humidity level. Once the target condition was reached, it was maintained for 3 hours. This cycle was repeated continuously over a period of 28 days.

#### Digital portable microscopy

A Dino-Lite® microscope (model AM4815ZT) was used to capture surface microscopy images. All photographs were processed using Dino-Lite® software, with the scale consistently indicated graphically.

The images obtained enabled the documentation of various crack patterns and degradation phenomena of the painting and facilitated the analysis of their distinct morphologies.

# Multiband technical imaging (MBI)

Multiband imaging is a well-established method widely utilized for heritage studies <sup>42–44</sup>, proving particularly effective for the analysis of paintings. <sup>45,46</sup>. A cross-sectional reading of the multiband images tends to provide a better understanding of the painting's execution process, revealing procedural and material data, which contribute to a deeper comprehension of conservation aspects. This is attributed to the specific behavior exhibited by some materials used in paint across the visible, ultraviolet, and infrared bands. Among other applications, the multiband imaging technique has been employed for the preliminary identification of pigments in works of art <sup>47,48</sup>. Lately, MBI has been useful to assess the correlation between pigments and their interaction with several forms of damage in paintings <sup>41,49</sup>.

λ= 300- 400 n

**ACRONYM** NAME SPECTRAL RANGE VIS Visible Visible Image (VIS) λ= 400-700 nr RL Raking light IR Infrared Infra Red Image (IR) λ= 1100 nr IRT Infrared transmitted light λ= 1100 nn TL Transmitted light UVL Ultraviolet-induced luminescence Visible Image (VIS) Reflected Ultraviolet UVR

Table 3 | List of acronyms representing different bands of the spectrum considered and their corresponding spectral areas

Among the several multiband and multimodal techniques, reflected ultraviolet (UVR), ultraviolet-induced visible luminescence (UVL), visible photography (VIS), transillumination (TL), infrared photography (IR), and infrared trans-irradiation (IRT) have been considered by their potential usefulness in this study. The list of acronyms and their spectral area is given in Table 3.

A Nikon® D800 camera (36 MP, CMOS sensor, sensitivity range 300–1100 nm) modified for full-spectrum digital imaging, equipped with a Nikon Nikkor 50 mm 1:1 lens, was used. The CHSOS Robertina® 52 mm filter set was used to capture different types of images. Two 800 W halogen lamps with diffusers were used for VIS and IR imaging. A single 800 W lamp was positioned 80 cm behind the canvas and was used in transillumination and trans-irradiation techniques. A CHSOS Fabrizio UV high flux 365 nm LED lamp was used for UVL and UVR imaging. A CHSOS card incorporating an AIC PhD card with pigmentary additions responsive in the IR and UV bands was used to calibrate the reflected images. Images were captured in RAW format and color-corrected using white balance based on the N8 neutral grey of the AIC card. Fixed exposure settings were applied: N8 150 s  $\pm$  5 for VIS, 100 s  $\pm$  5 for IR, and 50 for UVR, with the same grayscale used for corrections across all imaging modes.

#### Field emission scanning electron microscope (HR-FESEM)

HR-FESEM analyses were performed on cross-sections using a GeminiSEM 500 scanning electron microscope equipped with an EDX detector (Oxford Instruments) and a ZEISS ULTRA 55 system. The analysis aimed to investigate the interactions at the interface between the acrylic ground layers and oil paints. Thus, cross-sections of the multi-layered structures were obtained with a professional fiber microtome and then fixed with carbon tape to a metal plate in a parallel way. Only a few micrometers of the cross-section extended beyond the vertical plate, and this exposed portion was

coated with carbon. During the analysis, the type of coating used was indicated to the software to ensure that the coating did not interfere with the examination of the organic component.

The analysis was conducted in two modes:

- Point dot mode: Used for the semi-quantitative detection of elements.
- Mapping mode: Utilized to define the elemental distribution over a region of 133× magnification, employing an accelerating voltage of 10 keV.

A backscattered electron in-lens detector (EsB) was used, providing a pure backscattered signal without secondary electron contamination, ensuring very low acceleration potential. This detector offered high atomic number (Z) contrast and was uniquely capable of selecting electrons based on their energy, enabling the differentiation of elements with minimal atomic number differences.

# Attenuated total reflectance Fourier-transform infrared spectrophotometry (ATR-FTIR)

Infrared spectrophotometry analysis was conducted in ATR mode, to identify the composition of the paint materials and degradation products on the surface of the samples  $^{50}$ . Attenuated total reflectance Fourier-transform infrared (ATR-FTIR) spectra were acquired using a Bruker Optics Alpha spectrophotometer in ATR mode, equipped with a diamond crystal capable of probing a sample area of 0.75 mm with a penetration depth of  $\sim 1 \ \mu m$ .

The spectrometer featured a Pt/SiC globar source, a RockSolid interferometer with gold mirrors, and a deuterated triglycine sulphate (DLaTGS) detector, operating at room temperature and providing a linear response across the spectral range of 7500 to 375 cm<sup>-1</sup>. Spectra were recorded in the range of 4000 to 400 cm<sup>-1</sup>, with 48 scans performed at a resolution of 4 cm<sup>-1</sup>.

Data collection was managed using the Opus software, while spectra processing was carried out using Origin 9 and ThermoNicolet's OMNIC 6.0.

#### Gas chromatography-mass spectrometry (GC-MS)

GC-MS analysis was conducted on samples to determine the composition of binding media, the presence of organic additives, and any oxidation or degradation products.

The procedure adhered to a specialized protocol for modern and contemporary oil paints developed at the Ca' Foscari University: all details, experimental conditions and molar ratios considered for this study, are reported in previous studies<sup>19,40,41,49</sup>.

# **Results**

This section presents a detailed discussion of the data obtained from the combined use of a multi-analytical approach of non-invasive techniques, such as multiband imaging and portable digital microscopy, with microinvasive methods including HR-FESEM-EDX, ATR-FTIR, and GC-MS.

# Observation of degradation phenomena by means of noninvasive techniques

This section focuses on the visual and diagnostic examination of degradation patterns using non-invasive methods such as multiband imaging and digital microscopy.

Multiband imaging (MBI) was carried out to observe the surface and the possible alterations affecting paintings. VIS, RL, IR, IRT, TL, UVL, and UVR were used to record the appearance of the paintings across different bands of the spectrum and under different modes.  $^{41,45,49,51-53}$ .

Figures 2-4 show the images obtained using the different multiband techniques applied to SET3, SET2, and SET1, respectively. The images shown are a selection of the most relevant results.

The following degradation phenomena were observed in the prepared mock-ups by reading cross-sectionally and comparing several images taken:

- Wrinkles: uneven (small) folds, ridges or grooves resulting in an undulating and wavy layer on the paint surfaces<sup>54,55</sup>;
- Cracks: single cracks or networks of straight or slightly curved lines, known as craquelure<sup>49,56,57</sup>.
- Protrusions: tiny, translucent, or opaque white globules that break through the surface of the paint layer (protruding masses). Typically ranging from 50 to 300 µm in size—though they can be larger—these protrusions create a cratered texture on the surface.<sup>58-61</sup>.

Figure 2 collects the most interesting cases of SET3. The VIS and RL images show severe wrinkling. Considering that the samples kept at controlled room conditions also showed this alteration, it might be logical to think that the formation of wrinkles was not necessarily induced by the environment, but more likely related to the chemical composition of the paint films and/or the interaction between the paint and the preparatory layers. RL also allowed the cracks on the surfaces of the mock-ups to be better observed. Of particular interest are the mock-ups SET3-TiGD-T and SET3-ZnMM-T.

The observation of the surface morphology by optical microscopy (Fig. 3) revealed more pronounced and deeper cracks in the mock-ups with a zinc-based oil paint film. In such specimens, IR imaging showed darker cracks, suggesting that they also affected the inner layers<sup>62</sup>. In contrast, the mock-ups with a titanium-based oil paint film showed no light absorption, indicating that the cracks were more superficial and only affected the paint film (Fig. 4). The IR images were compared to IRT images, which provided additional information such as structural defects (voids, internal cracks, delamination or thermal changes caused by layers not visible in IR)<sup>51,53</sup>. By comparing the cracks of the three types of mockups studied, it was possible to distinguish between surface cracks (affecting only the paint film) and cracks with cleavage (affecting several layers and showing a separation between the paint film and the preparatory layers, although the paint film was still attached to the underlying substrate). The results confirmed the previous hypothesis: only the specimens made with

a zinc-oil paint film showed deep cracks with some degree of cleavage affecting the underlying layers.

This time-dependent process of crack propagation across the layers was determined by comparing the VIS, IR, and IRT images of the sample SET3-ZnMM-T. As shown in Fig. 5, neither the surface level captured in the VIS image nor the deeper level revealed in the IR image shows any cracks in the highlighted red area. However, the IRT technique highlights internal cracks in the layer closest to the canvas. The IRT image makes it possible to suppose that the cracks originate specifically in the acrylic primer before they become visible and propagate into the acrylic gesso (detected by IR) or the oil paint layer (detected by VIS).

Specific literature states that IRT images are sensitive to inhomogeneities, including trapped moisture or variations in material properties, which might alter the thermal behavior of painted surfaces<sup>63</sup>. The acquired IRT images allowed to observe areas where heat was not uniformly absorbed, resulting in darker areas. This initial observation was confirmed by TL images, where a halogen light source is positioned behind the canvases at a distance of 80 cm, and a sensitive camera records the light uniformly transmitted through it<sup>64</sup>. The quantity and quality of the light passing through depend on the thickness of the material. This technique allows the detection of defects or structural variations in the layers closest to the canvas, which would otherwise remain invisible on the surface.

In particular, in samples where darker areas were observed in IRT images, a similarly irregular surface is also visible in TL images. According to the literature, this phenomenon can be attributed to areas of different densities, aligning with previous observations<sup>64</sup>.

IRT and TL images also suggested a significant alteration in the thermal and optical properties of some mock-ups, indicating localized changes in their composition and condition.

These alterations are observed not only in SET3 but also in SET2 and SET1. Specifically, the results observed in samples SET3-ZnGD-RH%, SET2-TiGD-RH% and SET1-ZnMM-RH% were particularly relevant. These mock-ups exhibited thermal and optical inhomogeneity spots areas: accumulation of moisture (which appeared darker in TL and exhibited different thermal behavior in IRT images), corresponding to protrusion areas observed in VIS. Moreover, the combination of these techniques evidenced structural defects and forms of degradation not yet evident on the surface in the visible range. The aggregation of material that had not yet migrated to the surface in the form of protrusions observed in SET3-ZnMM-NAT seems to originate in the preparatory layers (Fig. 8).

Two forms of three-dimensional failure were registered in Fig. 9:

- · protrusions (as previously described);
- protrusions with medium separation: the separation and accumulation
  of the lipid medium in punctiform areas of the paint surface, forming a
  (locally) shiny, yellowish spot.

Such a degradation phenomenon is not always visible in the commonly reflected VIS photography. Instead, it can be better recorded by UVL imaging, which reveals features that were not evident under visible lighting conditions <sup>65–67</sup>, In the studied examples, UVL allowed to clearly distinguish between protrusions and protrusions with medium separation. In the three mock-ups under examination (SET3-ZnGD-RH%, SET2-TiGD-RH% and SET1-ZnMM-RH%), it was observed that (Fig. 10):

- the protrusions exposed to UV radiation showed a reflection phenomenon in correspondence to all the areas with protrusions;
- only the protrusions with medium separation reflect and emit light in the VIS spectrum, showing the luminescence nature of the lipid medium. Such luminescence is highly material-specific and depends on the chemical composition of the surface<sup>68</sup>.

In Fig. 3d, e show that oil separation also occurred within some of the cracks. This is confirmed by the luminescence response within the crack in UVL observed in SET3-ZnMM-T.

Finally, UVR analysis allowed the determination of specific characteristics related to the surface and chemical composition of the materials. UVR is the equivalent to IR and VIS reflected photographs, but in the UV band. An opaque effect was observed on the surface of the

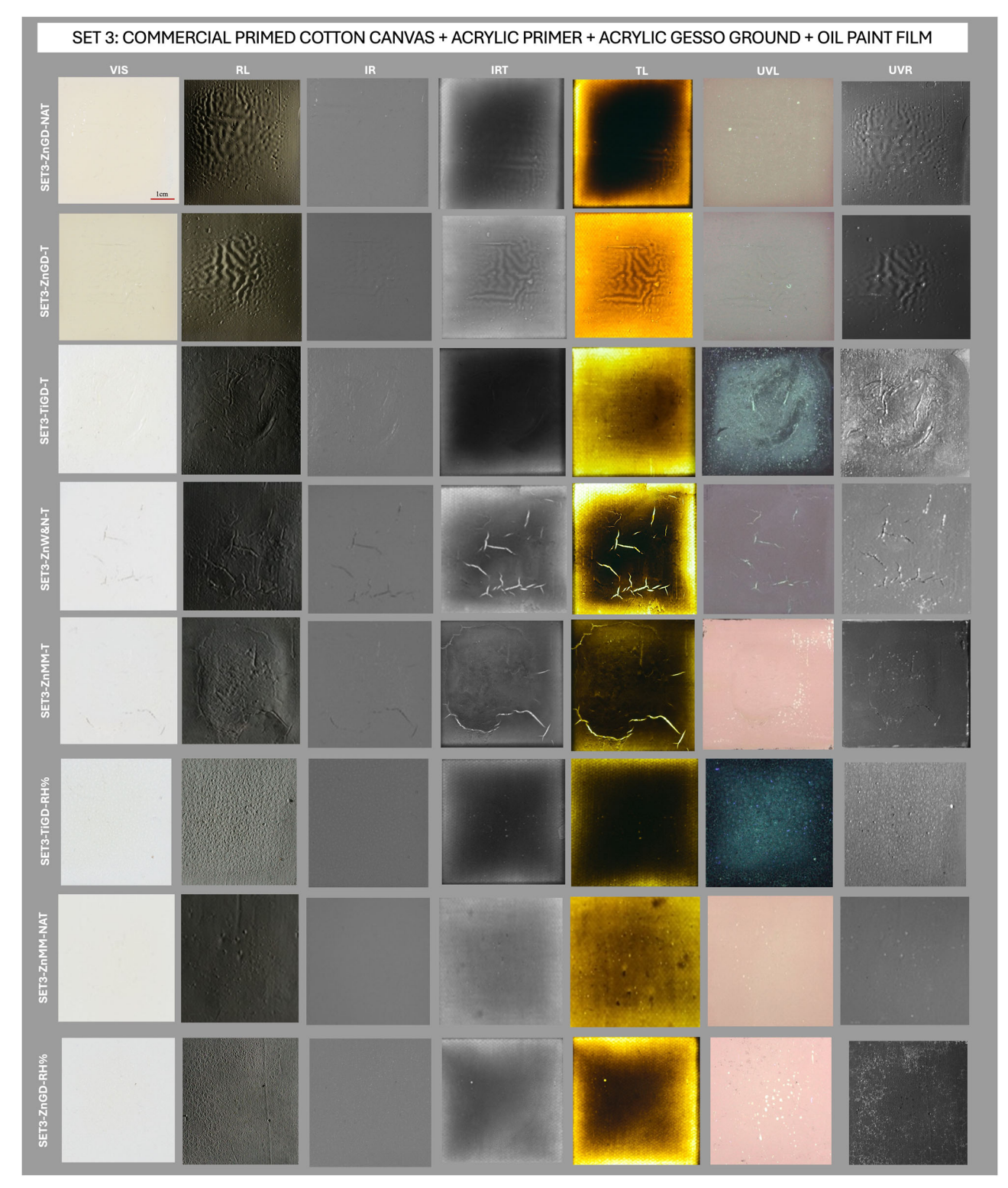


**Fig. 2** | Selected results of multiband imaging carried out in SET3 (commercial primed cotton canvas + acrylic primer + acrylic gesso ground + oil paint film). The images report only the central area of the canvas and exclude the area in contact with

the wooden stretcher. T: subjected to artificial ageing with a variation of temperature. RH%: subjected to artificial ageing with fluctuation of % relative humidity (RH%). NAT: subjected to natural ageing at room temperature.

mock-ups containing a Golden titanium white oil paint film in SET3 and SET2, and subjected to both natural and %RH artificial ageing. This could indicate either the presence of materials with high UV reflectance or scattering properties or a surface alteration. Due to the

interaction of UV radiation with materials, this technique highlights alterations such as photodegradation, usually not visible in VIS light or other spectral bands, which provides valuable information about the condition of the mock-ups.

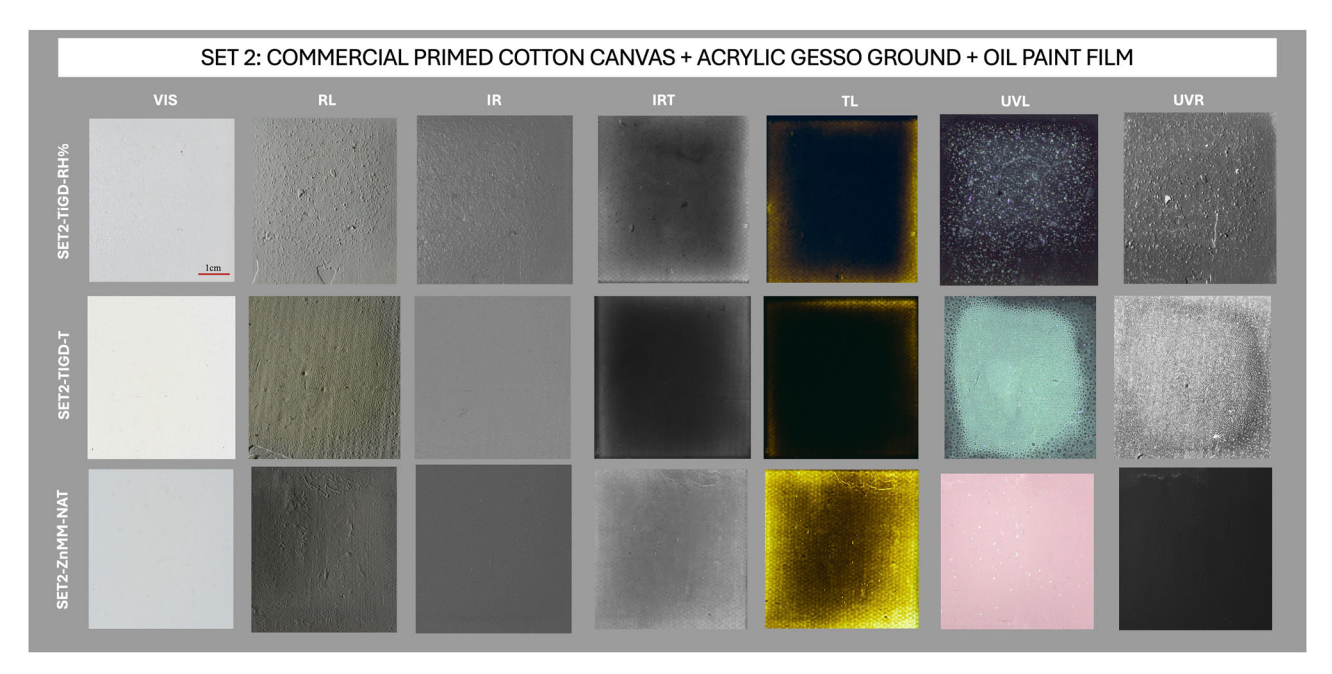


**Fig. 3** | Selected results of multiband imaging carried out in SET2 (commercial primed cotton canvas + acrylic gesso ground + oil paint film). The images report only the central area of the canvas and exclude the area in contact with the wooden

stretcher. T subjected to artificial ageing with a variation of temperature. RH% subjected to artificial ageing with fluctuation of % relative humidity (RH%). NAT subjected to natural ageing at room temperature.

# Chemical and physical interactions at the interface inbetween layers

This section focuses on the characterization of those samples that showed the most relevant failure issues at the interface between the acrylic preparatory layer and the oil paint film by means of noninvasive techniques.

SET1-ZnMM-RH% and SET3-ZnGD-RH% were selected to represent the mock-ups having protrusions which, in some cases, also showed medium separation (Fig. 9). In order to study these phenomena in detail, HR-FESEM-EDX was carried out, allowing a micro-morphological examination of the alteration and the detection of elements<sup>30</sup>. Cross-sectional analysis of the samples revealed two different types of protrusions: - protrusions with separation of the (lipid) medium (Fig. 11); - protrusions where the separation consists of metal soaps (Fig. 12).

Figure 11 shows the cross-section of SET1-ZnMM-RH% in the area corresponding to the protrusion and the separation of the medium previously observed in VIS on the surface. The analysis provided detailed insights into the structure of the mock-up and the distribution of elements in the organic components (carbon and oxygen) and the inorganic materials (zinc, calcium, magnesium, titanium, aluminium, sodium, and silicon) within the paint film.

The imaging revealed:

- a homogeneous distribution of zinc, sodium and calcium ions in the paint film;
- a distinct region, corresponding to the protrusion, where this homogeneity was disrupted, and only organic components were detected.

EDX confirmed the exclusive presence of carbon and oxygen, indicating that the region was basically composed of an organic compound, i.e., lipid medium, without any metal ions.

Figure 12 shows the analysis of SET3-ZnGD-RH%. As in the previous example, the cross-section was taken from an area where lipid medium separation was observed on the surface in the visible (VIS) band. The VIS image revealed a distinct region corresponding to the protrusion, enriched not only with carbon and oxygen—characteristic of the oil medium—but also with a significant concentration of zinc metal ions. The EDX spectrum confirmed the higher presence of an organic fraction along with metallic ions originating from the acrylic primer layer.

The samples in Figs. 11, 12 exhibit several common characteristics: • Both displayed a degradation mechanism involving the separation of the lipid fraction.

- Both contained a Zn-based paint layer, a pigment known to promote this type of deterioration.
- Both underwent artificial ageing with % RH fluctuations, a process that accelerates hydrolysis and the migration of metal ions. The key difference lies in the forms of degradation observed:
- in SET1-ZnMM-RH%, the separation consisted exclusively of the oil medium.
- in SET3-ZnGD-RH%, the separation involved an accumulation of organic material and zinc ions, which are probably related to the formation of metal soaps, a structure composed of metal ions present in the paint layer and free fatty acids from the lipid binder.

GC–MS and ATR-FTIR investigated the chemical interactions that led to the degradation phenomena observed  $^{50,63,69-71},\,$ 

The TIC (total ion current) chromatograms show all the characteristic fatty acids (as their corresponding methyl esters) detectable in oil paint films. Table S1, supplementary material, summarises the results of qualitative and quantitative analyses performed with GC–MS on the following mock-ups:

- SET3-ZnMM-T, which showed cracks with lipid medium separation;
- SET3-TiGD-T, which showed surface cracks;
- SET3-ZnGD-RH%, which showed protrusions probably consisting of metal soaps.
- SET1-ZnMM-RH%, which showed surface protrusions without lipid medium separation.

Figure 13 presents a focused wavelength region of the ATR spectrum and GC–MS chromatogram of sample SET3-ZnGD-RH%.

The spectra analyzed presented the characteristic bands of an oil binder:

- the broadband centered at ca. 3440 cm<sup>-1</sup> is assigned to the stretching of alcohol and hydroperoxide bonds;
- the band at ca.1740 cm<sup>-1</sup> assigned to the ester stretching;
- the bands corresponding to the CH stretching are ca. 2928 and ca. 2860 cm<sup>-1</sup>.

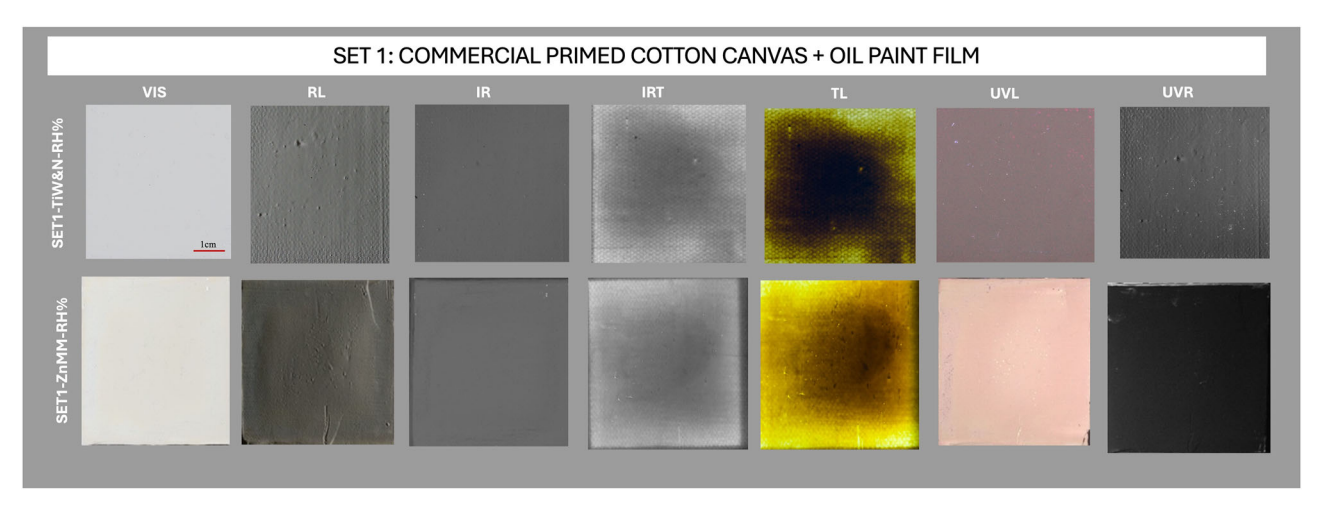


**Fig. 4** | Selected results of multiband imaging carried out in SET1 (commercial primed cotton canvas + oil paint film). The images report only the central area of the canvas and exclude the area in contact with the wooden stretcher. T subjected to

artificial ageing with a variation of temperature. RH% subjected to artificial ageing with fluctuation of % relative humidity (RH%). NAT subjected to natural ageing at room temperature.

ATR-FTIR analysis highlighted:

- the band at 1710 cm<sup>-1</sup> corresponding to the C=O stretching vibration related to the formation of carboxylic acids, which may form as a result of both the hydrolysis and oxidative degradation of triglycerides.
- Moreover, a broad band at ca.1580 cm<sup>-1</sup> related to amorphous zinc carboxylates was detected, since the band is shifted by 40 cm<sup>-1</sup> toward higher wavenumbers with respect to the absorptions of their corresponding crystalline Zinc soaps at ca. 1540 cm<sup>-172</sup>.
- Finally, the peaks at 1465–1464 m (CH $_2$   $\delta$  bending) and 1399–1397 m (symmetric carboxylate stretching  $\nu$  COO), due to the presence of carboxylate groups.

Overall, these features support the presence of non-crystalline zinc carboxylates and carboxylic acid groups within the protrusions, but do not allow for a definitive identification of specific zinc soap species. Zinc carboxylates were detected in all mockups shown in Fig. 9, confirming that this degradation phenomenon occurs in both zinc- and titanium-based oil paints. Literature suggests that zinc has a strong tendency to bind with carboxylate groups, forming metal soaps<sup>33,35,36,73</sup>. This explains their presence in the titanium oil paint mock-ups, which contain a 10% mixture of zinc oxide.

GC–MS results highlighted the presence of a variety of oxidized acids (e.g. oxo, hydroxy-, and epoxy-octadecanoic acids) related to an advanced degree of oxidation of the unsaturated fatty acids present in the fresh oil: these compounds are formed through the oxidative pathway of unsaturated fatty acids during the propagation reactions of the oxidation process<sup>25–27,74,75</sup>. The evidence of degradation processes is also supported by the detection of dicarboxylic fatty acids, such as sebacic acid, suberic acid, and azelaic acid, which are known to be the tertiary oxidation products of unsaturated fatty acids<sup>37,60,76–79</sup>.

The palmitic to stearic acid ratios (P/S) were calculated to help in defining the kind of oil used  $^{19}$  and compared with the information about oils reported in the technical data of color tubes. It was, therefore, possible to confirm that Golden Artist Colors Inc. (GD) employs alkali-refined linseed oil (P/S  $0.9\pm0.3$ ). Linseed oil has typically a P/S ratio of approximately  $1.6\pm0.3$ , but in the SET3-TiGD-T and SET3-ZnGD-RH% samples, the P/S ratios were notably lower (0.95 and 0.8, respectively) (Table S1). This might be linked to the common addition of metal stearates as dispersion agents in oil manufacture. The alkali-refining process used to produce alkali-refined linseed oil (ARLO) is highly effective in purifying the oil, removing mucilages, phospholipids, and other impurities, and improving its drying properties  $^{74,80}$ . However, this refining process involves the addition of free

fatty acids that may have favored the formation of metal soaps, as observed in this sample.

Moreover, mock-up SET3-ZnGD-RH% exhibited a higher glycerol concentration compared to other samples with the same paint layer (ZnO) from the same brand (Golden) and subjected to the same accelerated ageing conditions (RH%), but with different ground structures. Specifically, the glycerol percentage was 16.26% in sample SET3-ZnGD-RH%, 5.25% in sample SET2-ZnGD-RH%, and 3.32% in sample SET1-ZnGD-RH%.

This suggests that mock-up SET3-ZnGD-RH% underwent increased hydrolysis of ester-glycerol bonds, leading to the formation of di-, mono-, and triglycerides, glycerol, and free fatty acids<sup>74,80</sup>. The enhanced formation of metal soaps observed in this sample can therefore be attributed to its structural composition rather than the alkaline refining process used to produce ARLO.

The formation of metal soap reflects extensive degradation processes in the mock-ups of SET3, which not only affect the oil paint film, but also appear to originate in the preparatory layers, as supposed by comparing RL and IRT images (Fig. 8).

As is known from the literature, coalescence is the process where acrylic-based polymers consolidate into a dense, compact structure 82,83. During this process, as water and other volatile compounds evaporate, the micrometer-sized polymer particles merge, forming a strong hexagonal, honeycomb-like polymer network. This creates a dense microstructure, crucial for the mechanical stability and integrity of the resulting acrylic paint film. This also occurs in the case of the acrylic ground used in this experiment. Ideally, coalescence would form a continuous polymer film once dried. However, in this case study, the coalescence of the polymer spheres leads to a polymer film with interstitial spaces, resulting in somewhat porous acrylic films with channels running along the walls of the hexagonally deformed particles. These pores are pathways for water to move in and out of the film. In addition, because acrylic films require hydrophilic, waterattracting additives to ensure compatibility with water, they will inevitably retain some water, even after appearing fully dry. Thus, residual moisture can accumulate in some areas of the interface between the oil paint film and the acrylic ground, making the polymer system more susceptible to hydrolysis, as the ester bonds remain exposed to water molecules 13,72,81. Moreover, environmental factors significantly influence drying: the fluctuation of %RH can promote water absorption into the acrylic layer, further increasing the risk of hydrolysis<sup>72,82</sup>.

These processes highlight the key role of both chemical composition and environment in influencing the degradation kinetics of oil paint systems when applied to acrylic grounds<sup>81,83</sup>.

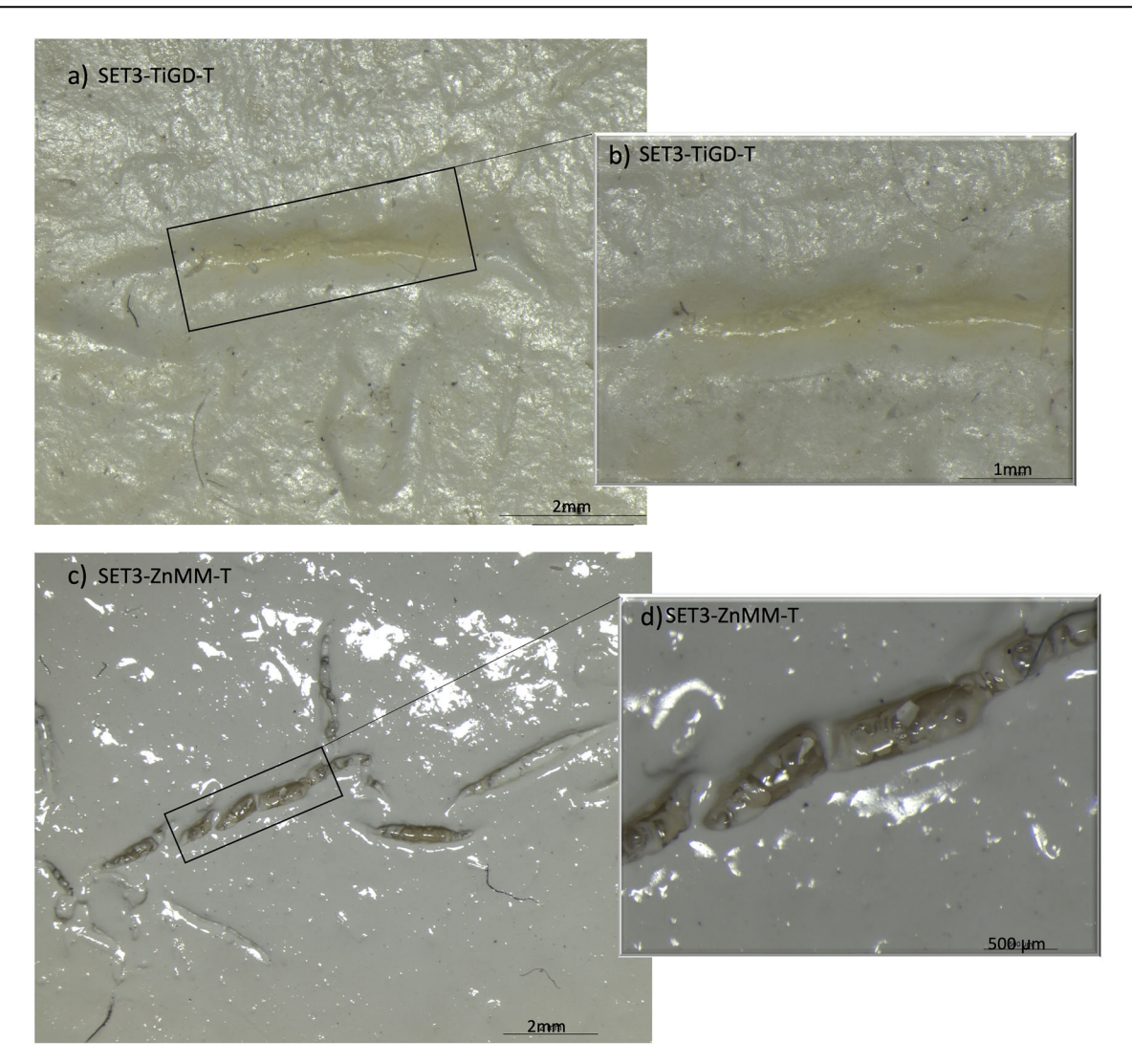


Fig. 5 | Crack patterns captured by digital portable microscopy. a A detailed view of the sample SET3-TiGD-T; b a closer examination of sample SET3-TiGD-T, revealing cracks on the surfaces; c a detailed view of the sample SET3- ZnMM-T; d higher magnification of sample SET3- ZnMM-T reveals deeper cracks with oil medium separation. TiGD titanium dioxide in rutile form from the brand Golden, ZnMM zinc oxide from the brand Maimeri, T subjected to artificial ageing with temperature variations.

Cross-sectional HR-FESEM-EDX images confirmed the observations made through optical microscopy (Fig. 3) and multiband imaging analysis (Figs.4,5):

- crack patterns were observed exclusively in samples from SET3;
- the different behavior of zinc and titanium white paint films under the same environmental conditions (artificial ageing with temperature variation) and the same structural composition (SET3).

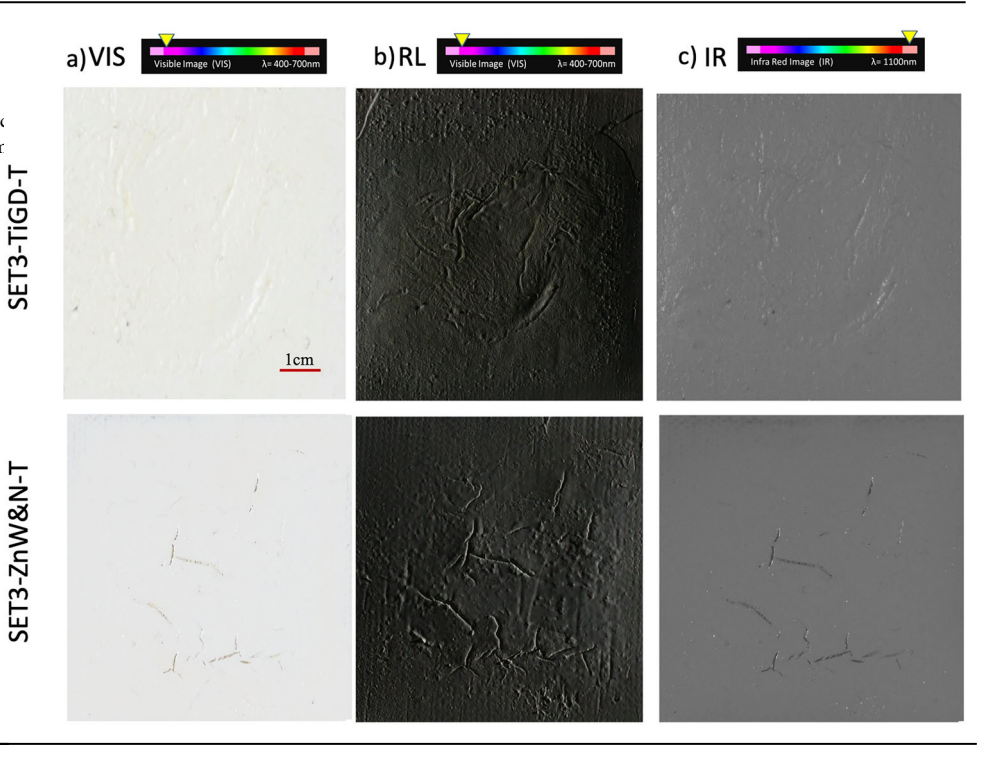
In Fig. 14, the cross-sectional analysis of the mock-ups with titanium white (SET3-TiGD-T) shows that the observed crack is exclusively confined to the paint film, thereby confirming the superficial nature of the cracks as previously described.

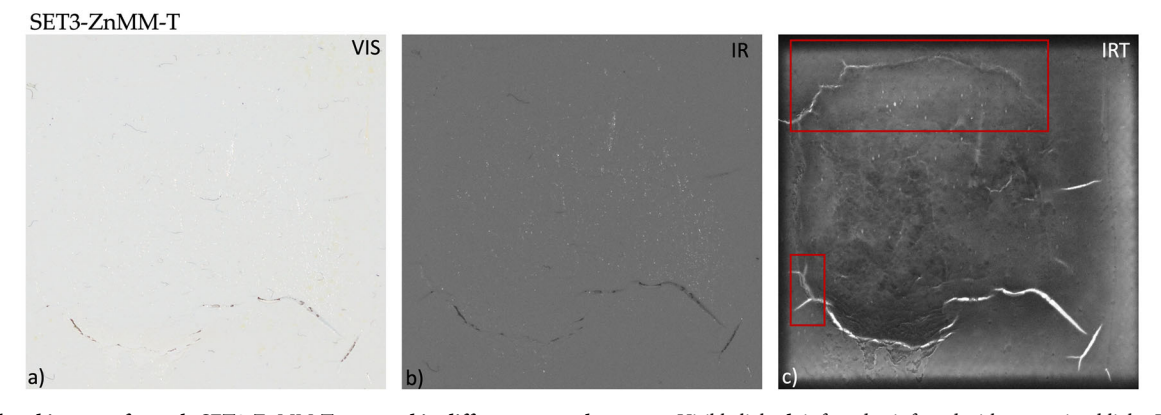
Figure 15 provides critical micro-scale insights into the structural damage and degradation mechanisms of the mockups made of a zinc-oil paint film (SET3-ZnW&N-T). Figure c highlights that the cracks start within the acrylic primer, traverse the entire acrylic gesso ground layer and terminate at the paint film. This observation is consistent with previous studies indicating that zinc oxide can reduce the flexibility of paint films, increasing the risk of cracking, delamination, and metal soap formation 33-37,73. In addition, the crack propagation through the layers from the bottom (acrylic primer) to the top (oil paint film) was demonstrated by comparing the VIS, IR, and IRT images of this sample. (Fig.5).

The damage observed in mock-ups made with a zinc white oil paint film is attributed to its chemical and mechanical properties. It is well known that zinc oxide forms a brittle and inelastic paint film. Furthermore, these properties are enhanced by the tendency of zinc ions to bind to the carboxylate groups of the polymer network, acting as anchor points for the carboxylic acid groups during the paint-drying process. This increases the density of cross-links and leads to a decrease in elastic properties over time, resulting in increased rigidity and brittleness. The brittleness of the paint film compromises its structural integrity, making it more susceptible to deeper friable cracking under stress. In contrast, the titanium white samples exhibited superficial cracks confined to the oil paint film, suggesting a more stable structural integrity<sup>18,78,84-87</sup>. It is known from the literature that titanium white does not form stiff films, but has limited strength and behaves in a somewhat flexible manner. This would explain the superficial cracking observed, which only affected the paint film, leaving the underlying ground layer intact, as acrylic films are more elastic. 17,81,84-87.

This distinction highlights the key role of pigments in the mid-to-long-term durability and stability of oil paintings. This study shows that the interaction between the pigmented oil medium at the interface with acrylic grounds may significantly govern some physical properties of the oil paint film, such as its flexibility, adhesion to the underlying substrate, and sensitivity to moisture (and environment fluctuations).

Fig. 6 | Multiband images of samples SET3-ZnW&N-T and SET3-TiGD-T were captured in different spectral ranges. a Visible light; b ranking light; c infrared. IR images show deeper cracks in zinc white oil paint film and superficial cracks in titanium white oil paint film.





 $\label{eq:continuous} \textbf{Fig. 7} \ | \ \textbf{Multiband images of sample SET3-ZnMM-T captured in different spectral ranges.} \ \textbf{a} \ \text{Visible light;} \ \textbf{b} \ \text{infrared;} \ \textbf{c} \ \text{infrared with transmitted light.} \ \text{In} \ (\textbf{c}), \ \text{cracks} \ \text{highlighted in red become visible,} \ \text{which were not detectable in the other images.}$ 

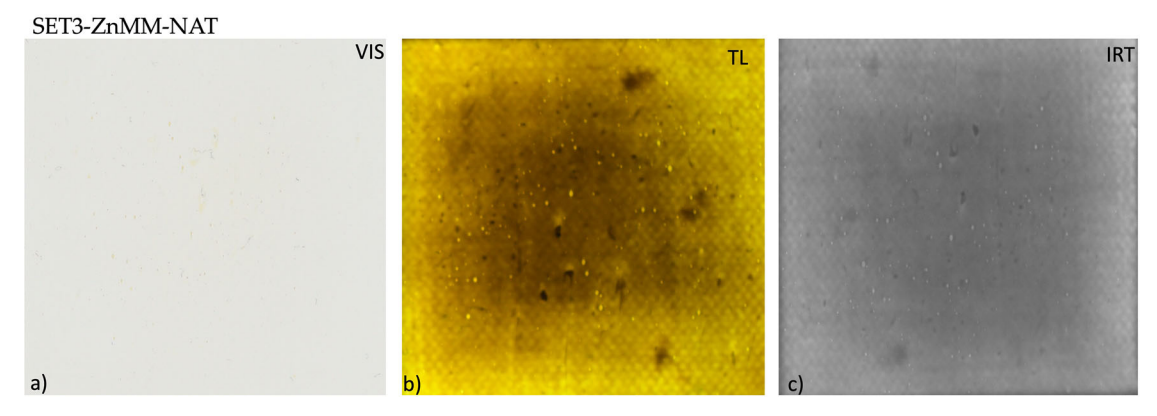
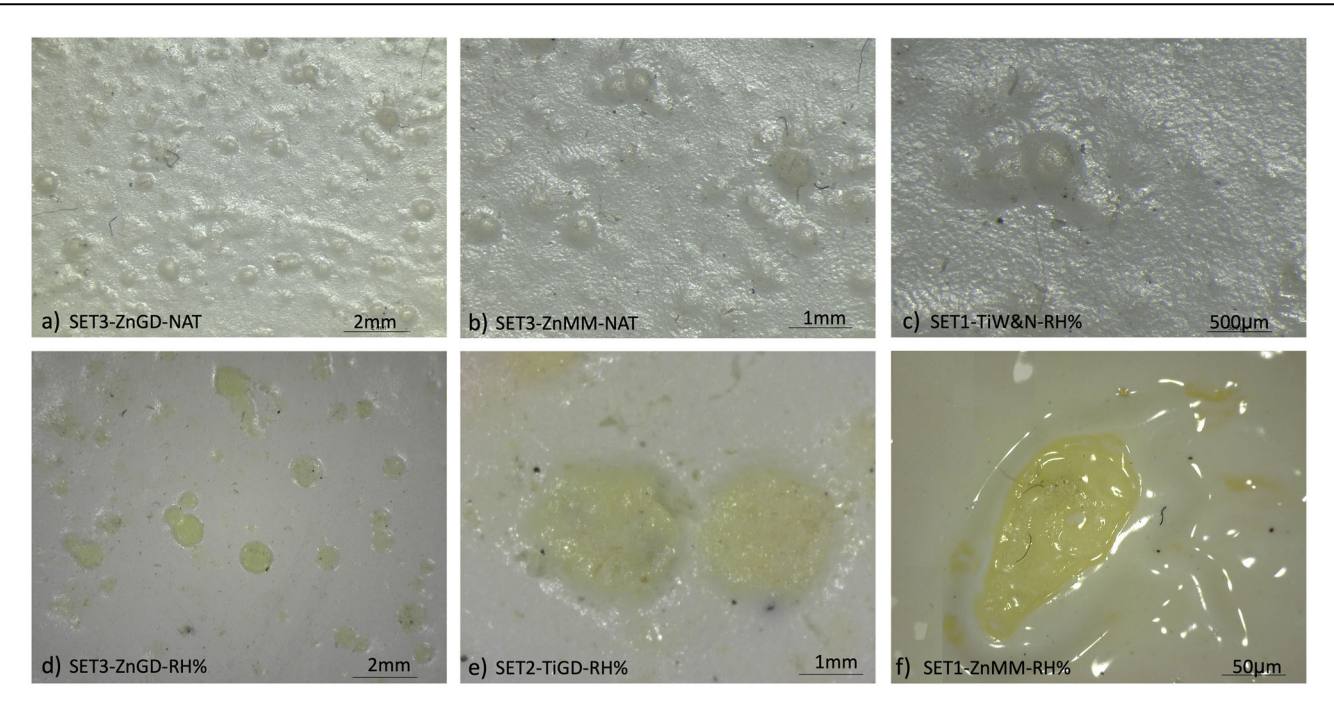


Fig. 8 | Multiband images of sample SET3-ZnMM-NAT captured in different spectral ranges. a Visible light; b transmitted light; c infrared with transmitted light. TL and IRT images revealed structural inhomogeneities which corresponded to protrusions areas not yet visible at naked eyes.



**Fig. 9 | Protrusions captured by digital microscopy. a** SET3-ZnGD-NAT; **b** SET3-ZnMM-NAT; **c** SET1-TiW&N-RH%; **d** SET3-ZnGD-RH%; **e** SET2-TiGD-RH%; **f** SET1-ZnMM-RH%. SET3 (commercial primed cotton canvas + acrylic primer + acrylic gesso ground + oil paint film). SET2 (commercial primed cotton canvas + acrylic gesso ground + oil paint film); SET1 (commercial primed cotton

canvas + oil paint film). Ti titanium dioxide in rutile form, GD golden, MM Maimeri, W&N Winsor & Newton, T subjected to artificial ageing with temperature variations. RH% subjected to artificial ageing with % relative humidity variations, NAT natural ageing at room temperature.

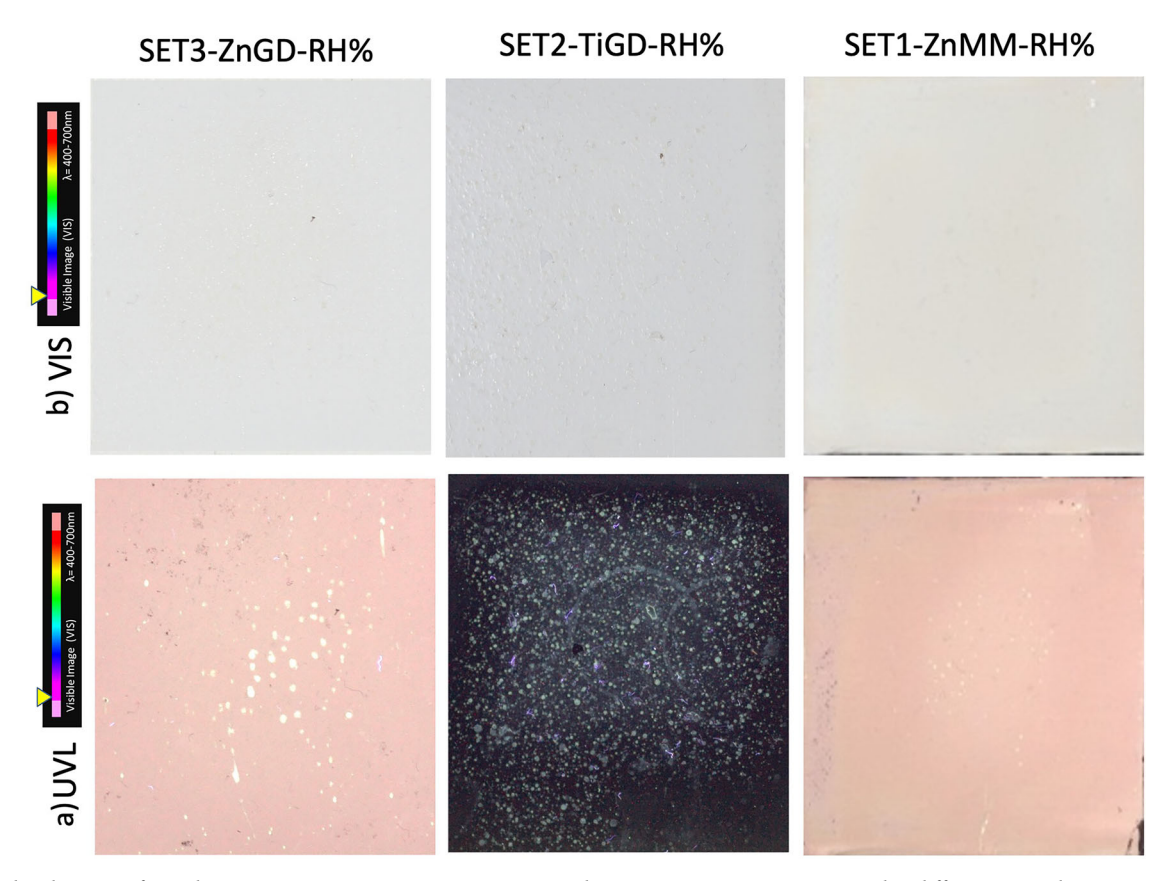


Fig. 10 | Multiband images of samples SET3-ZnMM-NAT, SET2-TiGD-RH% and SET1-ZnMM-RH% were captured in different spectral ranges. a Visible light; b ultraviolet-induced luminescence.

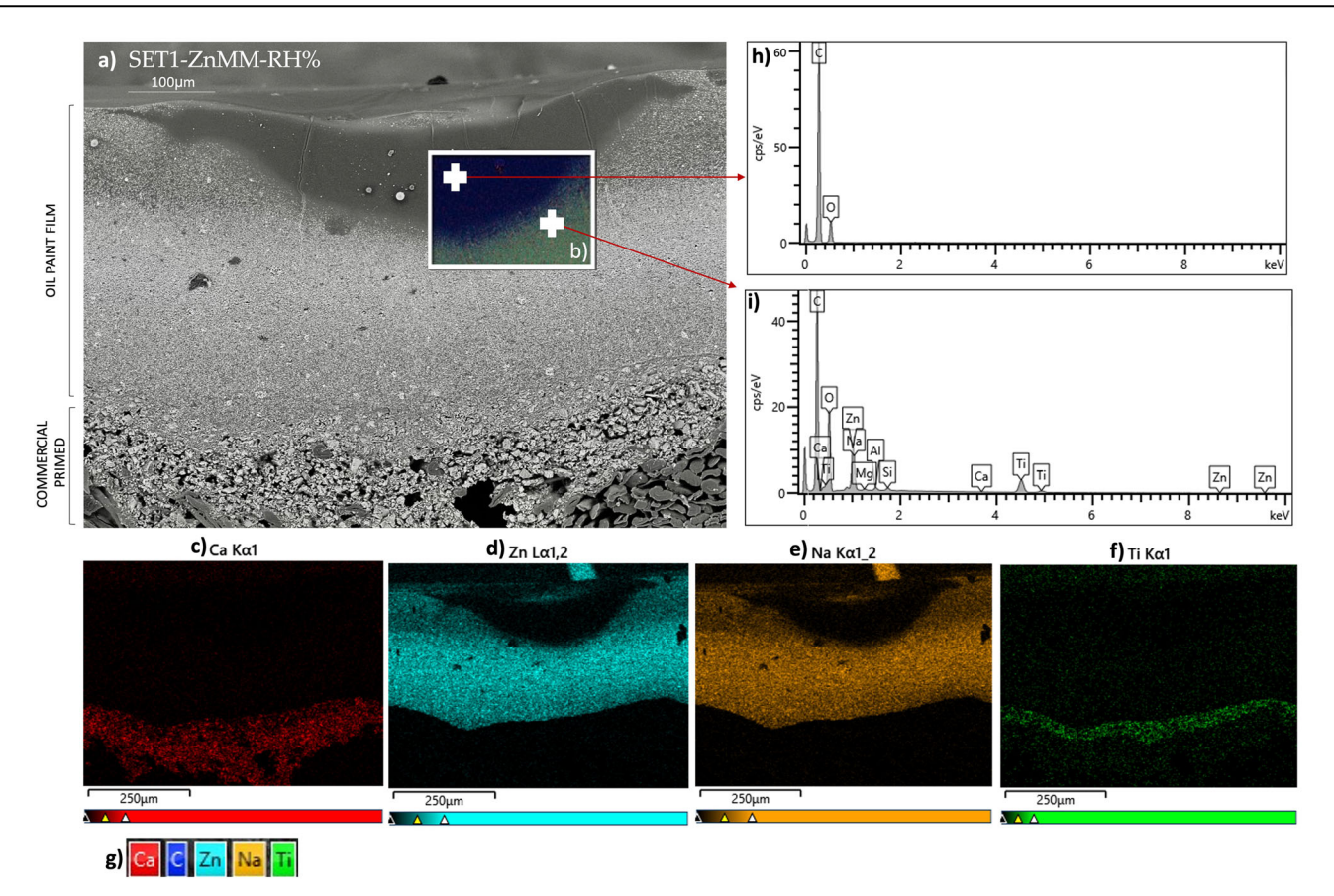


Fig. 11 | High-resolution field emission scanning electron microscopy (HR-FESEM) images and energy dispersive X-ray spectroscopy (EDX) mappings of protrusion patterns observed in SET1-ZnMM-RH%. a close-up of the protrusion with lipid medium separation visible on the paint layer surface; b elemental mapping of all detected elements in a specific area of the examined cross-section; c distribution mapping of calcium ions across the selected area; d distribution mapping of zinc ions

across the selected area; **e** distribution mapping of sodium ions across the selected area; **f** distribution mapping of titanium ions across the selected area; **g** color legend of elements in maps; **h** elemental spectrum acquired at the protrusion site with lipid medium separation; **i** elemental spectrum acquired from the paint layer region. SET1 (commercial primed cotton canvas + oil paint film.). Zn zinc paint layer, MM brand Maimeri, RH% subjected to artificial ageing with % relative humidity variations.

### **Discussion**

This research provides a comprehensive analytical protocol capable of identifying, localizing and characterizing early degradation phenomena at the interface between acrylic preparatory layers and oil paint films in contemporary oil paintings. The use of representative mock-ups-designed based on a survey of Italian artists—and carefully selected ageing conditions, makes the study highly relevant to real-world painting practices and the challenges encountered in modern art conservation. Multiband imaging techniques proved to be a valuable non-invasive tool for detecting the early stages of physico-chemical degradation in mock-ups, allowing intervention before damage is visible on the painted surface. By comparing multiband images, it was possible to distinguish the surface alterations from inner ones and to understand the crack propagation process across the layers. RL images helped to identify and document wrinkling and cracking. The combined use of RL with IR images provided a more detailed analysis by allowing surface cracks in the paint film to be distinguished from deeper cracks that affect several layers and showed a separation between the paint film and the preparatory layers (cleavage).

Cross-sectional HR-FESEM-EDX images confirmed that crack patterns were present only in SET3, reinforcing the idea that the interactions taking place at the interface between the oil paint film and the acrylic preparatory layers have a dramatic impact on the physical stability of the composite painted system.

A different behavior was observed for zinc and titanium white paint films under the same environmental conditions (artificial ageing with temperature variation) and with the same layered structure (SET3). In mock-ups made of zinc white, the cracks start in the acrylic primer, pass through the entire acrylic gesso ground layer and end at the paint layer. This crack propagation process across the layers was determined by comparing the VIS, IR, and IRT images. These results suggest that such phenomena may be favored by the ability of zinc oxide to react with free fatty acids when incorporated into oil paints and to bind to the carboxylate groups of the polymer network, resulting in increased cross-linking capacity. This led to a fragile and brittle paint film more susceptible to deeper cracking under stress. In mock-ups with a titanium white oil paint film instead, cracking appeared to be confined exclusively to the paint film, confirming its weaker and more flexible behaviour.

IRT and TL images also revealed significant alterations in the thermal and optical properties of some mock-ups, suggesting localized accumulation of moisture.

- In acrylic grounds, two main factors may lead to moisture accumulation:
   non-ideal coalescence, which creates a somewhat porous acrylic film, allowing water to penetrate through the pores.
- certain amount of hydrophilic or water-attracting additives that hold onto some water even after appearing fully dry, leading to moisture accumulation.

Thus, residual moisture can concentrate at the interface between the oil paint film and the acrylic ground, making the polymer system more susceptible to hydrolysis, as the ester bonds remain exposed to water molecules.

This phenomenon was particularly evident in the samples SET3-ZnGD-RH% and SET1-ZnMM-RH%, where these alterations were more pronounced. UVL allowed the preliminary differentiation between protrusions (thanks to its reflection phenomenon under UV) and protrusions

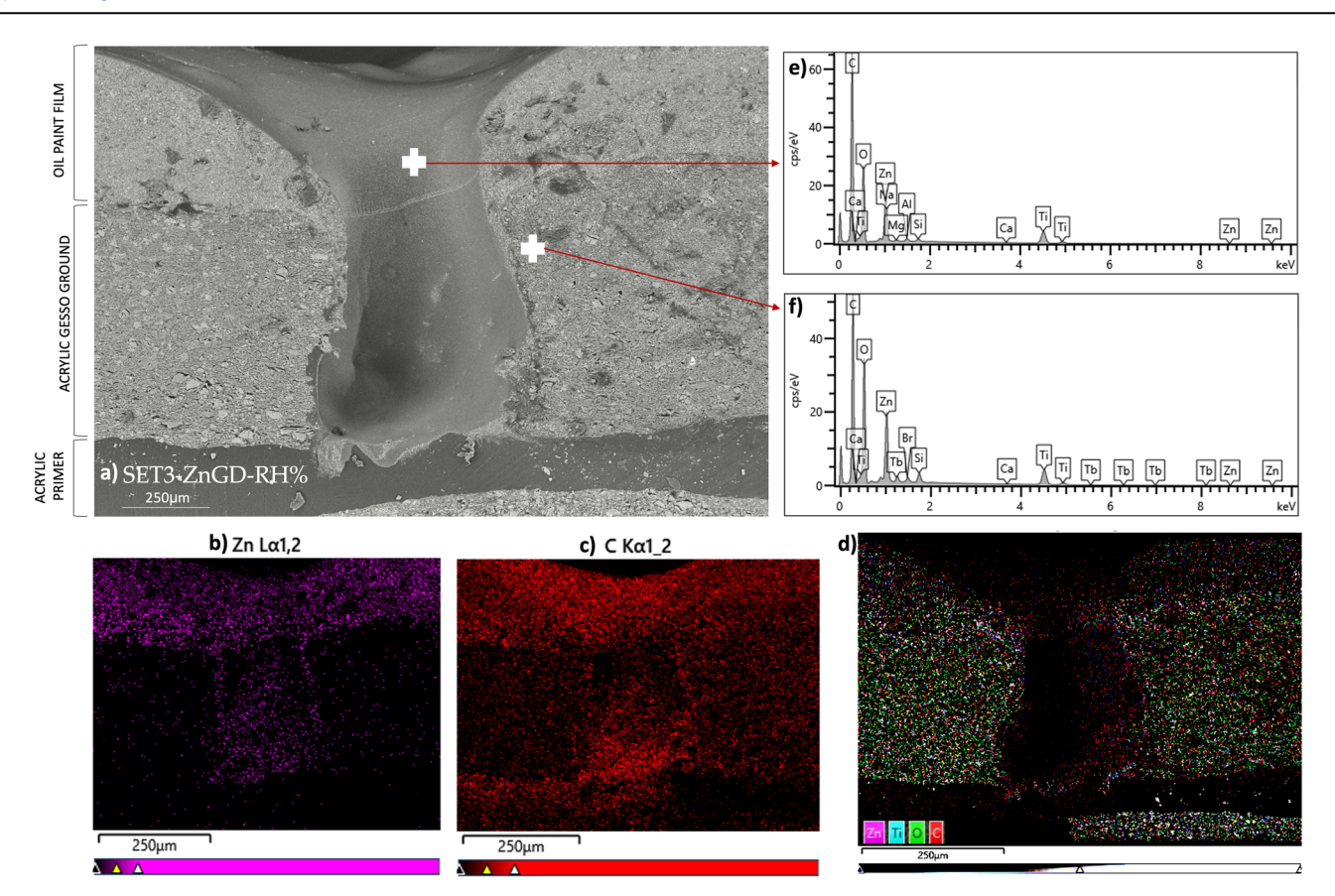


Fig. 12 | High-resolution field emission scanning electron microscopy (HR-FESEM) images and energy dispersive X-ray spectroscopy (EDX) mappings of protrusion patterns observed on mock-up SET3-ZnGD-RH%. a Close-up of a protrusion; b distribution mapping of zinc ions across the selected area; c distribution mapping of carbon ions across the selected area; d elemental mapping of all detected elements in a specific area of the examined cross-section; e elemental

spectrum acquired at the protrusion site with lipid medium separation; **f** elemental spectrum acquired from the paint layer region. SET3: (consisting of pre-primed canvas, acrylic primer, acrylic ground gypsum, paint layer). Zn zinc paint layer, GD brand Golden Artist Color Inc, RH% subjected to artificial ageing with relative humidity percentage variations.

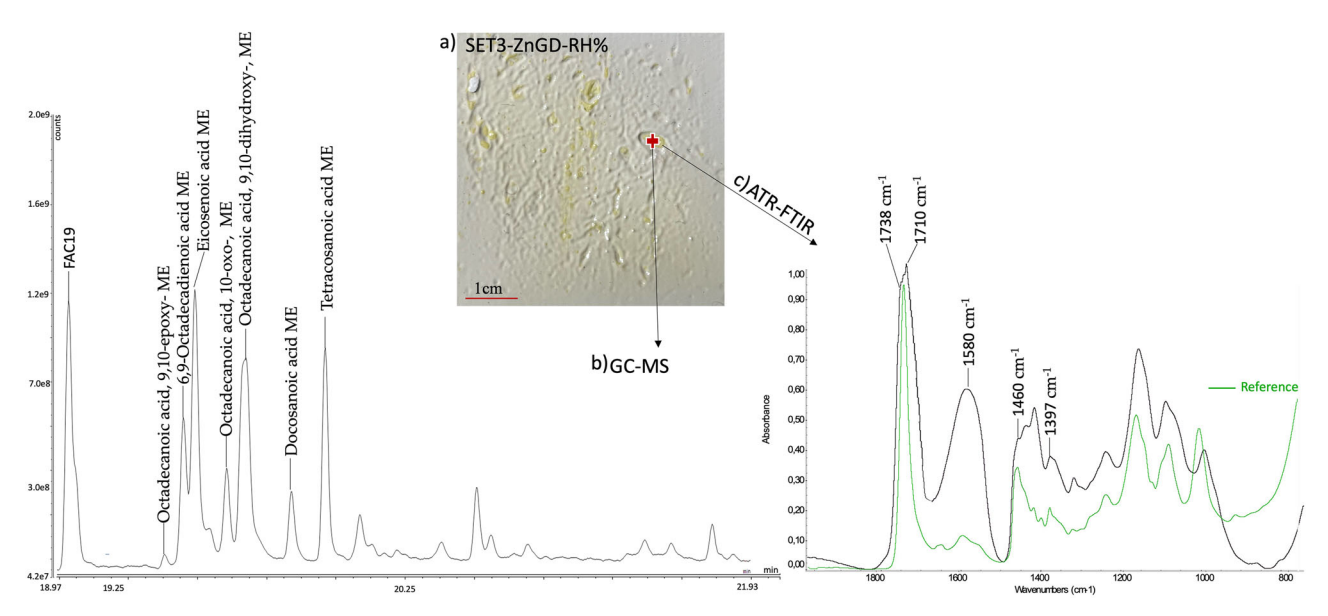


Fig. 13 | Summary of GC-MS and ATR-FTIR analysis on mock-up SET3-ZnGD-RH%. a Close-up of the sample, with the point of analysis marked by red crosses; b Chromatogram with relevant peaks concerning the presence of oxidated

compound; c spectrum showing relevant peaks indicating the presence of carboxylic acid and non-crystalline zinc carboxylates (black), compared to the spectrum of the mock-up 1 h after casting as a reference (green).

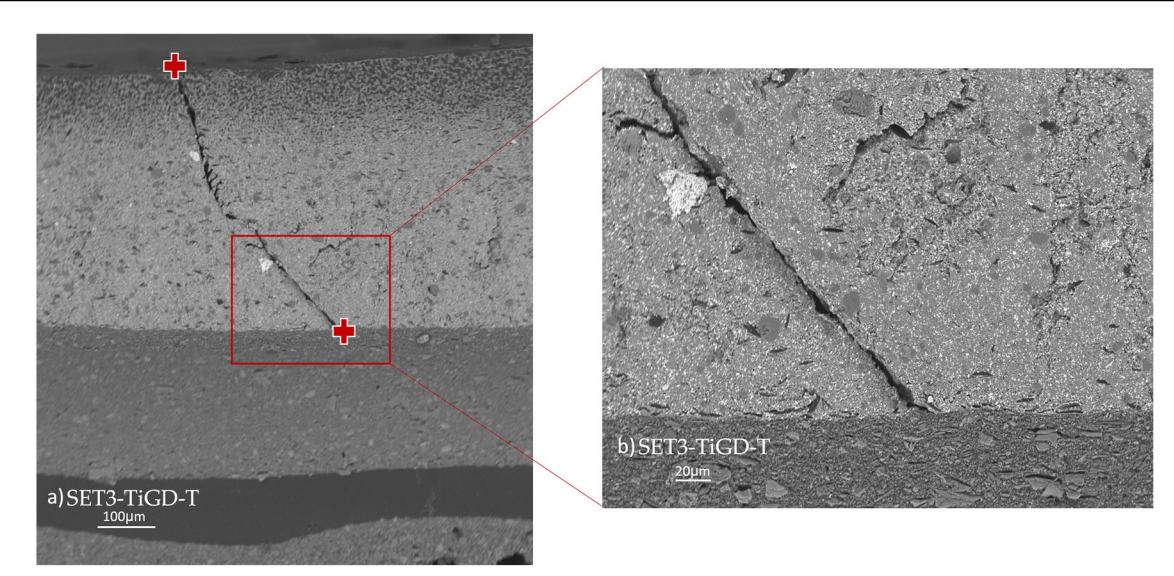


Fig. 14 | High-resolution field emission scanning electron microscopy (HR-FESEM) images of cracks pattern observed on mock-up SET3-TiGD-T. a Close-up of a crack limited in the paint layer, with the start and end points marked by red crosses; b 20  $\mu$ m magnification of the interface between the paint layer and the

acrylic gesso ground layer, showing the end of the crack. SET3: (consisting of preprimed canvas, acrylic primer, acrylic ground gypsum, paint layer). Ti titanium paint layer, GD brand Golden Artist Color Inc., T subjected to artificial ageing with temperature variations.

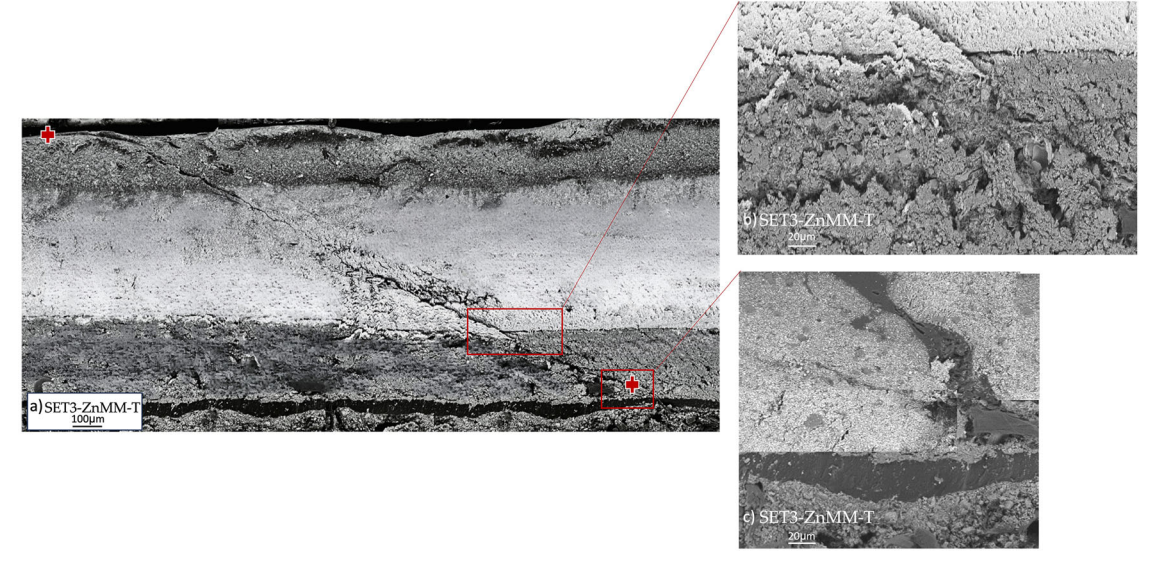


Fig. 15 | High-resolution field emission scanning electron microscopy (HR-FESEM) images of cracks pattern observed on mock-up SET3-ZnMM-T. a Close-up of a crack with the start and end points marked with red crosses; b 20  $\mu m$  magnification of the interface between the oil paint film and the acrylic gesso ground;

c 20  $\mu$ m magnification of the interface between the acrylic gesso ground and the acrylic primer. SET3: (consisting of pre-primed canvas, acrylic primer, acrylic ground gypsum, paint layer). Ti titanium paint layer, GD brand Golden Artist Color Inc., T subjected to artificial ageing with temperature variations.

with medium separation (which emitted light in the visible spectrum). Moreover, the application of HR-FESEM-EDX allowed a micromorphological examination of these protrusions to be carried out, which made it possible to identify when the separation was exclusive of the oil medium, and when it also involved metal ions. In addition, the spectroscopic analysis identified non-crystalline zinc carboxylates. Using advanced analytical techniques such as GC–MS, the chemical interactions responsible for the observed degradation phenomena were thoroughly investigated. The presence of various oxidized acids suggested advanced oxidation of unsaturated fatty acids and the high degree of hydrolysis of ester-glycerol bonds was further supported by the detection of elevated concentrations of dicarboxylic acids and glycerol. An interesting comparison can be made with the study by Romano et al. 88, who analyzed medium-rich protrusions in

zinc white oil paint and identified crystalline zinc carboxylates, with higher zinc concentrations in the center and lower levels toward the edges. In our samples, although no crystalline zinc soaps were detected, the absence of inorganic elements in the center of the protrusions and their accumulation at the edges suggests a potentially different distribution dynamic. These differences highlight the need for further investigation into how local composition, pigment type, and aging conditions influence the formation and spatial organization of such degradation features.

These results evidence how informative the integration of multiband imaging with advanced analytical techniques can be in understanding the degradation mechanisms involved in painted systems that combine an oil paint film applied to an acrylic substrate, as well as in identifying degradation phenomena at a very early stage that would otherwise not be detectable before they become visible to the naked eye.

The samples that exhibited the most significant chemical-physical issues were those from SET3, which consisted of an oil paint layer by Golden and Maimeri brands applied over ground layers by W&N. In contrast, only a few samples from SET3, featuring an oil paint layer by W&N, showed conservation problems. This suggests that, beyond the interface issues between the acrylic ground and the oil paint layer discussed in the article, the compatibility of additives may also play a crucial role. Or, in other words, paintings made by combining materials from the same given brand seem to present a higher compatibility and stability (and therefore less tendency to degradation) than those where grounds and paint films are from different brands.

Future research will specifically focus on this aspect by applying the presented analytical approach, which has proved to be an effective method of identifying degradation phenomena commonly found in modern and contemporary paintings such as wrinkles, protrusions, and cracks. These findings are important for both artists and conservators, as they highlight the need for an understanding of material interactions to make informed choices of painting materials in order to mitigate the long-term degradation of paintings.

#### **Data availability**

Data supporting the findings of this study are available from the corresponding author, upon reasonable request.

Received: 30 December 2024; Accepted: 4 June 2025; Published online: 23 July 2025

# References

- 1. Borgioli, L. I Leganti Nell'arte Contemporanea (Nardini Editore, 2020).
- Stols, M. in *Grounds* 1400–1900 (eds J. Hill Stoner, R. Rushfield) (London, Routledge, 2012).
- 3. Jo, C. & Tom, L. The Impact of Modern Paints (Watson-Guptill, 2000).
- Izzo, F. C., Balliana, E., Pinton, F. & Zendri, E. A preliminary study of the composition of commercial oil, acrylic and vinyl paints and their behaviour after accelerated ageing conditions. *Conserv. Sci. Cult. Herit.* 14, 353–369 (2014).
- Whitmore, P. M. & Colaluca, V. G. The natural and accelerated aging of an acrylic artists' medium. Stud. Conserv. 40, 51–64 (1995).
- Learner, T. J. S. Analysis of Modern Paints. Research in Conservation (The Getty Conservation Institute, 2005).
- 7. Learner, T. J. S., Smithen, P., Krueger, J. W. & Schilling, M. R. *Modern Paints Uncovered* (The Getty Conservation Institute, 2008).
- Genestar, C. Characterization of grounds used in canvas and sculpture. Mater. Lett. 54, 382–388 (2002).
- Dodiuk, S. K. H. The effect of surface preparation on the performance of acrylic adhesive joints. *Int. J. Adhes. Adhes.* 8, 159–166 (1988).
- Pratali, E. Zinc oxide grounds in 19th and 20th century oil paintings and their role in picture degradation processes. CeROArt (2013).
- Chiantore, O., Scalarone, D. & Learner, T. Characterization of artist' acrylic emulsion paints. *Int. J. Pol. Anal. Charact.* 8, 67–82 (2003).
- Burnstock, A., Ormsby, B., Schar, M. & Carlyle, L. Drying and oxidative degradation of linseed oil. Conservation of modern oil paintings. *Polym. Degrad. Stab.* 65, 303–313 (2019).
- Cooper, A., Burnstock, A., Van der Berg, K. J. & Ormsby, B. in Issue in Contemporary Oil Paint (eds Van der Berg, K. J. et al.) (Springer, 2013).
- Ormsby, B., Hodgkins, R. E. & von Aderkas, N. Preliminary investigation into two new acrylic emulsion paint formulations: W&N artists' acrylic colours and golden open acrylics. e-Preserv. Sci. 9, 9–16 (2012).
- Izzo, F. C., Van Den Berg, K. J., Van Keulen, H., Ferriani, B. & Zendri, E. Issues in Contemporary Oil Paint (Springer International Publishing, 2014).

- Izzo, F. C., Balliana, E., Perra, E. & Zendri, E. Accelerated ageing procedures to assess the stability of an unconventional acrylic-wax polymeric emulsion for contemporary art. *Polymers* 12, 1925 (2020).
- Lee, D. S. H. Numerical modelling of mechanical degradation of canvas paintings under desiccation. *Herit. Sci.* 10, 1–13 (2022).
- van Driel, B. A. et al. Determination of early warning signs for photocatalytic degradation of titanium white oil paints by means of surface analysis. Spectrochim. Acta A Mol. Biomol. Spectrosc. 172, 100–108 (2017).
- Izzo, F. C. 20th Century Artists' Oil Paint: A Chemical-Physical Survey.
   PhD thesis, University of Ca' FoscariUniversity (2011).
- Maor, Y. & Murray, A. Delamination of oil paints on acrylic grounds. Mater. Res. Soc. Symp. Proc. 1047, 127–136 (2008).
- Ortiz Miranda, A. S., Kronkright, D. & Walton, M. The influence of commercial primed canvases in the manifestation of metal soaps protrusions in Georgia O'Keeffe's oil paintings. *Herit. Sci.* 8, 1–15 (2020).
- 22. Salvant, J. et al. in *Metal Soaps in Art Conservation and Research* Springer International Publishing, 2019).
- Ploeger, R., Scalarone, D. & Chiantore, O. The characterization of commercial artists' alkyd paints. J. Cult. Herit. 9, 412–419 (2008).
- 24. Mallegol, J., Lemaire, J. & Gardette, J. Drier influence on the curing of linseed oil. *Prog. Org. Coat.* **39**, 107–113 (2000).
- Juita, B., Dlugogorski, E. Z., Kennedy, E. & Mackie, J. Oxidation reactions and spontaneous ignition of linseed oil. *Proc. Combust. Inst.* 33, 2625–2631 (2011).
- Tumosa, C. S. & Meckelnburg, M. F. Weight changes on oxidation of drying and semi-drying oils. Collect. Forum 18, 116–123 (2003).
- Pizzimenti, S. et al. Oxidation and cross-linking in the curing of airdrying artists' oil paints. ACS Appl. Polym. Mater. 3, 1912–1922 (2021).
- Cotte, M. Lead soaps in paintings: friends or foes?. Stud. Conserv. 62, 2–23 (2017).
- 29. Tumosa, C. S. & Mecklenburg, M. F. The influence of lead ions on the drying of oils. *Stud. Conserv.* **50**, 39–47 (2005).
- Chen-Wiegart, Y. C. K. et al. Elemental and molecular segregation in oil paintings due to lead soap degradation. Sci. Rep. 7, 1–9 (2017).
- Keune, K. & Boon, J. J. Analytical imaging studies of cross-sections of paintings affected by lead soap aggregate formation. *Stud. Conserv.* 52, 161–176 (2007).
- 32. Watson, G. Revisiting Oils Over Acrylics, Just Paint (Golden Artist Color Inc., 2022).
- 33. Osmond, G. in Metal Soaps in Art. Cultural Heritage Science (Springer, 2019).
- 34. Artesani, A. Zinc oxide instability in drying oil paint. *Mater. Chem. Phys.* **255**, 123640 (2020).
- 35. Beerse, M., Keune, K., Iedema, P., Woutersen, S. & Hermans, J. Evolution of zinc carboxylate species in oil paint ionomers. *ACS Appl. Polym. Mater.* **2**, 5674–5685 (2020).
- 36. Palladino, N. An analytical survey of zinc white historical and modern artists' materials. *Herit. Sci.* **12**, 1–29 (2024).
- Giorgi, L. In-situ technical study of modern paintings Part 2: imaging and spectroscopic analysis of zinc white in paintings from 1889 to 1940 by Alessandro Milesi (1856–1945). Spectrochim. Acta A Mol. Biomol. Spectrosc. 219, 504–508 (2019).
- Sawicka, L., Izzo, F. C., Van der Berg, K. J. & Burnstock, A. in Issues in Contemporary Oil paint, book of Abstract (Cultural Heritage Agency, Ministry of Education, Culture and Science, 2013).
- 39. Nardelli, F. The stability of paintings and the molecular structure of the oil paint polymeric network. *Sci. Rep.* **11**, 1–14 (2021).
- Izzo, F. C. et al. Selective damage induced by pigment-medium interactions in a neoplasticist oil canvas painting: composition dans le cône avec couleur orange by G. Vantongerloo (1929). Herit. Sci. 12 (2024).

- 41. Gnemmi, M., Fuster-Lòpez, L. & Mecklenburg, M. Ion migration mechanisms in the early stages of drying and degradation of oil paint films. *npj Mater. Degrad.* **8**, 63 (2024).
- Cosentino, A. A practical guide to panoramic multispectral imaging. e-Conserv. Mag. 25, 64–73 (2012).
- 43. Cosentino, A., Caggiani, M. C., Ruggiero, G. & Salvemini, F. Panoramic multispectral imaging: training and case studies. *Belgian Bulletin*, **2nd Trimester** 7–11 (2014).
- 44. Webb, E. K., Summerour, R. & Giaccai, J. in *Textile Group Postprints* (AIC, 2014).
- Herrero-Cortell, M. A., Raich, M., Artoni, P. & Madrid Garcia, J. A. Caracterización de pigmentos históricos a través de técnicas de imagen, en diversas bandas del espectro electromagnético. Ge-Conserv. 22, 58–75 (2022).
- Herrero-Cortell, M. A., Creus, M. R. & Artoni, P. Multi-band technical imaging in the research of the execution of paintings. The case study of the portrait of Carlos IV, by Francisco de Goya. *Geconserv.* 14, 5–15 (2018).
- Cosentino, A. Identification of pigments by multispectral imaging; a flowchart method. *Herit. Sci.* 2, 8 (2014).
- Barnu, O. & Zahariade, Z. Noninvasive in situ study of pigments in artworks by means of VIS, IRFC image analysis, and X-ray fluorescence spectrometry. Col. Res. Appl. 41, 3 (2016).
- Fuster-López, L. et al. Selective cracks: mapping damage from pigment-medium interaction in three neo-plastic oil paintings. In: Working Towards a Sustainable Past. ICOM-CC 20th Triennial Conference Preprints, Valencia (ICOM-CC, 2023).
- Berthomieu, C. & Hienerwadel, R. Fourier transform infrared (FTIR) spectroscopy. *Photosynth. Res.* 101, 157–170 (2009).
- Herrero-Cortell, M., Artoni, P. & Raïch, M. Transmitted light imaging in VIS and IR, in the study of paintings: a brief report on the behavior of the main historical pigments. *Color Cult. Sci.* 12 (2020).
- Frey, J. et al. The AIC Guide to Digital Photography and Conservation Documentation (American Institute for Conservation of Historic and Artistic Works. 2017).
- Herrero Cortell, M. À et al. Observando a través de los estratos: fotografía infrarroja transmitida (IRT) aplicada al estudio técnico y documental de pinturas sobre lienzo. Ge-Conservación 19, 62–73 (2021).
- McMillan, G., Casadio, F., Fiedler, I. & Sorano-Stedman, V. An investigation into Kandinsky's use of Ripolin in his paintings after 1930, J. Am. Inst. Conserv. 52, 258–277 (2013).
- Casadio, F. Interdisciplinary investigation of early house paints: Picasso, Picabia and their 'Ripolin' paintings. In ICOM-CC 16th Triennial Meeting Postprints (Critério Artes Gráficas, Lda.; ICOM Committee for Conservation, 2011).
- Bosco, E., Suiker, A. S. J. & Fleck, N. A. Crack channelling mechanisms in brittle coating systems under moisture or temperature gradients. *Int. J. Fract.* 225, 1–30 (2020).
- Giorgiutti-Dauphiné, F. & Pauchard, L. Painting cracks: a way to investigate the pictorial matter. J. Appl. Phys. 120, 065107 (2016).
- 58. Steele, L. L. Effect of certain metallic soaps on the drying of raw linseed oil. *Ind. Eng. Chem.* **16**, 957–959 (1924).
- Casadio, F. et al. Metal Soaps in Art: Conservation and Research (Springer International Publishing, 2018).
- Izzo, F. C., Kratter, M., Nevin, A. & Zendri, E. A critical review on the analysis of metal soaps in oil paintings. *ChemistryOpen* 10, 904–921 (2021).
- 61. Hermans, J. J., Keune, K., Van Loon, A. & Iedema, P. D. in *Metal Soaps in Art* (eds Casadio, F. et al.) (Springer, 2019).
- Thoury, M. et al. Near-infrared luminescence of cadmium pigments: in situ identification and mapping in paintings. *Appl. Spectrosc.* 65, 939–951 (2011).
- Matteini, M. A. Moles, applications of trasmitted infrared radiation to the examination of artifacts. Stud. Conserv. 30, 1–10 (1983).

- 64. Cucci, C. et al. Trans-illumination and trans- irradiation with digital cameras: Potentials and limits of two imaging techniques used for the diagnostic investigation of paintings. *J. Cult. Herit.* **13**, 83–88 (2012).
- 65. Burrafato, G. et al. ColoRaman project: Raman and fluorescence spectroscopy of oil, tempera and fresco paint pigments. *J. Raman Spectrosc.* **35**, 879–886 (2004).
- Isacco, E. & Darrah, J. The ultraviolet-infrared method of analysis, a scientific approach to the study of Indian miniatures. *Artibus Asiae* 53, 470 (1993).
- Cosentino, A. Practical notes on ultraviolet technical photography for art examination. *Conservar Património* 21, 53–62 (2015).
- López, L. F., Stols-Witlox, M. & Picollo, M. UV-Vis Luminescence Imaging Techniques/Técnicas de imagen de luminiscencia UV-Vis (Universitat Politècnica de València, 2020).
- Moutsatsou, A., Skapoula, D. & Doulgeridis, M. The contribution of transmitted infrared imaging to non-invasive study of canvas paintings at the National Gallery – Alexandros Soutzos Museum, Greece. E-Conserv. Mag. 22, 53–61 (2011).
- López-Ramírez, M. R., Navas, N., Rodríguez-Simón, L. R., Otero, J. C. & Manzano, E. Study of modern artistic materials using combined spectroscopic and chromatographic techniques. Case study: painting with the signature 'Picasso. *Anal. Methods* 7, 1499–1508 (2015).
- 71. Vila, A. et al. in *Conservation of Modern Oil Paintings* (eds van den Berg, K. et al.) Ch. 18 (Springer, 2019).
- Banti, D. A molecular study of modern oil paintings: Investigating the role of dicarboxylic acids in the water sensitivity of modern oil paints. RSC Adv. 8, 6001–6012 (2018).
- Osmond, G. Zinc white: a review of zinc oxide pigment properties and implications for stability in oil-based paintings. AICCM Bull. 33, 20–29 (2012).
- Modugno, F. et al. On the influence of relative humidity on the oxidation and hydrolysis of fresh and aged oil paints. Sci. Rep. 9, 1–16 (2019).
- Costantini, R., Balliana, E., Dalla Torre, D., Aricò, F. & Zendri, E. Evaluating the impacts of alcohol-based solutions on silk: chemical, mechanical and wettability changes before and after artificial ageing. *Heritage* 5, 3588–3604 (2022).
- Izzo, F. C., Källbom, A. & Nevin, A. Multi-analytical assessment of bodied drying oil varnishes and their use as binders in armour paints. Heritage 4, 3402–3420 (2021).
- Giorgi, L. et al. In-situ technical study of modern paintings part 1: The evolution of artistic materials and painting techniques in ten paintings from 1889 to 1940 by Alessandro Milesi (1856–1945). Spectrochim. Acta A Mol. Biomol. Spectrosc. 219, 530–538 (2019).
- van Driel, B. New insights into the complex photoluminescence behaviour of titanium white pigments. *Dyes Pigments* 155, 14–22 (2018).
- Gomez Lobon, M. et al. A study of cadmium yellow paints from Joan Miró's paintings and studio materials preserved at the Fundació Miró Mallorca. Herit. Sci. 11, 1–16 (2023).
- Costantini, R., Nodari, L., Nasa, J. L. & Tomasin, P. Relative humidity, light, and inorganic fillers: defining different roles on the ageing of modern oil paints through infrared spectroscopy, *Microchem. J.* 208, 112534 (2024).
- Hagan, E. & Murray, A. Effects of water exposure on the mechanical properties of early artists' acrylic paints. *Mater. Res. Soc. Symp. Proc.* 852, 41–47 (2005).
- 82. Baij, L., Chassouant, L., Hermans, J. J., Keune, K. & ledema, P. D. The concentration and origins of carboxylic acid groups in oil paint. *RSC Adv.* **9**, 35559–35564 (2019).
- Hagan, E. W. S., Charalambides, M. N., Young, C. R. T. & Learner, T. J.
   S. The effects of strain rate and temperature on commercial acrylic artist paints aged one year to decades. *Appl. Phys. A Mater. Sci. Process* 121, 823–835 (2015).

- Santo, V. D. & Naldoni, A. Titanium dioxide photocatalysis. *Catalysts* 8, 591 (2018).
- 85. Curran, M. et al. The kinetics of fading: opaque paint films pigmented with alizarin lake and titanium dioxide. *J. Am. Inst. Conserv.* **23**, 114–129 (2018).
- Janas, A. et al. Mechanical properties and moisture-related dimensional change of canvas paintings-canvas and glue sizing. Herit. Sci. 10, 1–10 (2022).
- Janas, A., Mecklenburg, M., Fuster.Lopez, L. & Kozlowski, R. Shrinkage and mechanical properties of drying oil paints. *Herit. Sci.* 10, 1–10 (2022).
- 88. Romano, C., Lam, T., Newsome, G.A., Taillon, J.A., Little, N. & Little, J. Characterization of Zinc Carboxylates in an Oil Paint Test Panel. *Stud Conserv.* **65**, 14–27 (2020).

# **Acknowledgements**

The research is carried out as part of the National PhD in Heritage Science (PhD-HS.it). Curriculum: Arte contemporanea, Università degli Studi "Ca' Foscari" di Venezia, CUP 351: B53C22007260006, Missione: I.4.1 Borse PNRR Patrimonio Culturale (Missione 4), Componente: 1. F.C.I. acknowledges "Patto per Venezia" — Municipality of Venice for funding part of the instrumentation used for the characterisation of samples. Multiband studies have been carried out in the framework of Grant PID2023-148300NB-I00 funded by MICIU/AEI/ 10.13039/501100011033 and by "ERDF/EU". Finally, authors acknowledge Sofia Vicente and Eva Montesinos for their assistance in characterizing the fabrics used in this research.

#### Author contributions

Conceptualization, methodology, software and analyses, data curation, writing—original draft preparation, and project administration, M.G., L.F.-L., and F.C.I.; validation, investigation, and resources M.G., L.F.-L., F.C.I., M.A.H.-C., A.V.-E.; writing—review and editing, M.G., L.F.-L., F.C.I., M.A.H.-C., A.V.-E.; funding acquisition, M.G. L.F.-L., and F.C.I. All authors have read and agreed to the published version of the manuscript.

#### **Competing interests**

The authors declare no competing interests.

#### **Additional information**

**Supplementary information** The online version contains supplementary material available at https://doi.org/10.1038/s40494-025-01861-1.

**Correspondence** and requests for materials should be addressed to Laura Fuster-L-ópez or Francesca Caterina Izzo.

**Reprints and permissions information** is available at http://www.nature.com/reprints

**Publisher's note** Springer Nature remains neutral with regard to jurisdictional claims in published maps and institutional affiliations.

Open Access This article is licensed under a Creative Commons Attribution-NonCommercial-NoDerivatives 4.0 International License, which permits any non-commercial use, sharing, distribution and reproduction in any medium or format, as long as you give appropriate credit to the original author(s) and the source, provide a link to the Creative Commons licence, and indicate if you modified the licensed material. You do not have permission under this licence to share adapted material derived from this article or parts of it. The images or other third party material in this article are included in the article's Creative Commons licence, unless indicated otherwise in a credit line to the material. If material is not included in the article's Creative Commons licence and your intended use is not permitted by statutory regulation or exceeds the permitted use, you will need to obtain permission directly from the copyright holder. To view a copy of this licence, visit http://creativecommons.org/licenses/by-nc-nd/4.0/.

© The Author(s) 2025